2008

Biomechanical Evaluation Of Proximal Humerus Fracture Fixation And Rotator Cuff Repair

Parthasarathy Raghava
University of Alabama at Birmingham

BIOMECHANICAL EVALUATION OF PROXIMAL HUMERUS FRACTURE FIXATION AND ROTATOR CUFF REPAIR

by

PARTHASARATHY RAGHAVA

ALAN W. EBERHARDT, COMMITTEE CHAIR
BRENT A. PONCE
JACK E. LEMONS

A THESIS

Submitted to the graduate faculty of The University of Alabama at Birmingham
in partial fulfillment of the requirements for the degree of
Master of Science in Biomedical Engineering

BIRMINGHAM, ALABAMA

2008

BIOMECHANICAL EVALUATION OF PROXIMAL HUMERUS FRACTURE FIXATION AND ROTATOR CUFF REPAIR

Parthasarathy Raghava

BIOMEDICAL ENGINEERING

ABSTRACT

Locked plating is frequently used to treat proximal humerus fractures. However, varus collapse remains common. Anatomic reduction may decrease the frequency of varus collapse though no studies have evaluated this relation. Hence the first part of this study was to evaluate the role of calcar comminution and calcar fixation upon fixation stability.

Eleven matched humeri with three-part fractures were fixed with proximal humeral locking plate. Six pairs had an additional 1-cm medial wedge removed to simulate calcar comminution. Within each matched humerus, one had calcar fixation with long screws while the other did not. The constructs were then loaded to failure. Load and energy to failure, stiffness and displacement at failure were measured. A multivariate regression analysis was performed to evaluate the effect on the measurands.

The results showed that the non-comminuted specimens yielded 49% and 45% higher average load and energy to failure than comminuted specimens ($p<0.05$). Additionally, calcar fixation resulted in 22% and 27% higher load and energy values in comminuted and non-comminuted specimens respectively ($p<0.05$). The study suggested that calcar comminution critically destabilizes proximal humerus fractures while calcar fixation provides additional stability.

The second part of the project evaluates the properties of the lasso-loop stitch compared to simple, mattress, Modified Mason-Allen (MMA) and Massive-Cuff (MAC)

stitches that are used in rotator cuff repairs. Effect of three tissue penetrator geometries (clever hook, chia perc-passer and ideal suture passer) and tissue bite size (0.5-cm versus 1.0-cm) on suture strength was also evaluated.

One-hundred and twenty four sheep infraspinatus tendon were used. Each graft was first cyclically loaded and then loaded to failure. Peak to peak displacement, cyclic elongation and load to failure were measured. Two-way analysis of variance was employed to compare the different properties. The results showed that the lasso-loop stitch had similar failure values to the mattress stitch ($p=0.62$). No significant differences were found in the average load to failure between the different tissue penetrators ($p>0.05$). Also, a 1.0-cm purchase had a significantly higher failure load than the 0.5-cm bite size ($p<0.05$). In this study, three variable parameter were examined with the aim of improving suture-tendon strength.

DEDICATION

To my ever-loving parents, brother, family and my friends

for their constant and unconditional support throughout my life.

ACKNOWLEDGEMENTS

First, I would like to thank my advisor, Dr. Alan Eberhardt, for his great mentorship and guidance throughout my project. He not only made my graduate research really interesting but also made it enjoyable by providing me with a great level of freedom to work on my own. Next I thank Dr. Brent Ponce for helping me understand the concepts behind the shoulder arthroscopy. He was always ready to help me in spite of his very busy work schedule and was the driving force behind these projects. I also sincerely thank Dr. Jack Lemons for giving his time to serve on my committee and his valuable suggestions to improve my research work.

Next I would like to thank Dr. Kevin Thompson and Dr. Chad Hosemann for helping me with the dissection and preparation of the specimens for the biomechanical tests. I also thank Ms. Janet Tate for helping me with the statistical analysis. Thank to Girish Ramaswamy, who taught me to work on the MTS. Also sincere thanks to the administrative members, especially Razan, Toni and Thyrza for their encouragement and support.

I also would like to thank my parents, and my brother for providing the emotional support during the tough times. I am also grateful to Raja, Rajiv, Priya, Meenakshi, Rick, Mandar and others who have contributed in their own way to my success.

This project was funded by Synthes and Depuy Mitek.

TABLE OF CONTENTS

Page

CHAPTER Page

LIST OF TABLES

LIST OF FIGURES

Figure Page

Figure Page

LIST OF ABBREVIATIONS

ANOVA	Analysis of Variance
BMD	Bone Mineral Density
DEXA	Dual Energy X-ray Absorptiometry
ISP	Ideal Suture Passer
LCP-PHLP	Locking Compression Proximal Humerus Locking Plate
LL	Lasso Loop
MAC	Massive Cuff
MCL	Medial Comminuted with Long screws
MCS	Medial Comminuted with Short screws
MMA	Modified Mason-Allen
MTS	Materials Testing System
NCL	Non-comminuted with Long screws
NCS	Non-comminuted with Short screws
PHLP	Proximal Humerus Locking Plate

CHAPTER 1

INTRODUCTION

1.1 Proximal Humerus Fractures

The shoulder joint is the most mobile joint of the human body. It allows movement of the arm with respect to the thorax. Movements of the human shoulder involve a complex relationship of muscle forces, ligament constraints, and other bony articulations. Static and dynamic stabilizers allow the shoulder the greatest range of motion of any joint in the body. However this extensive range of motion is not without risk. If any of the static or dynamic stabilizers are injured by trauma or overuse, the shoulder is at increased risk for injury. Shoulder injuries account for 8% to 20% of athletic injuries (Steinbruck, 1999).

Proximal humerus fracture is the second most common fracture of the upper extremity, following distal forearm fracture. A survey by US Medicare population has found that fracture of the proximal humerus account for 10 percent of all fractures (Baron et al., 1996). In the United States alone, over 300,000 fractures of the proximal humerus occur annually (Praemer et al., 1992). Of these fractures, 80% are minimally displaced (<1 cm) and can be treated with early physical therapy (Neer, 2002). However, the rest 20% of the fractures have substantial displacement (>1 cm), or angulation (>45°), rotation, or tuberosity involvement. Closed reduction methods, particularly with comminuted, unstable two-part surgical neck patterns, have frequently led to poor clinical results because of the inability to gain and maintain a satisfactory reduction. Increasing attention

has been focused on operative fixation for unstable two/ three part surgical neck fractures, although there is controversy regarding the optimal fixation technique (Gardner et al, 2007).

Different techniques are used for internal fixation of displaced proximal humeral fractures. The most common devices include plate fixation, fixed-angle plate fixation, antegrade intramedullary fixation, tension-band wiring, percutaneous fixation, and external fixation (Agel et al., 2004). However, these devices have their own limitations. Inadequate implant fixation may result in implant loosening, fracture re-displacement, and poor patient outcome. In patients over sixty-five years old, the bone of the proximal aspect of the humerus is usually osteoporotic. Thus independent from the method chosen for fracture repair, reduced bone mass and bone quality of the humeral head complicate internal fixation (Bernard et al., 2000).

With the advent of locking fixation, a greater number of displaced proximal humerus fractures are being treated with locking plates. Locking plates have better mechanical and torsional stability than the conventional fixation techniques (Sara et al., 2006). However, despite the increased stability and use of locking fixation, loss of reduction remains a post-operative problem in comminuted, osteoporotic bone. One complication still seen, despite the added strength provided by the locked plate over conventional fixation, is hardware failure with collapse of the fracture into varus. One large series with proximal humerus locking plates had a 15-20% rate of varus collapse (Plecko et al., 2005; Owsley et al., 2006). A varus humeral head-shaft angle can compromise the shoulder

biomechanics. In varus collapse, the head-shaft angle is reduced from around 140 degrees to less than 120 degrees. This decrease in angle has been associated with pain and limited shoulder motion (Owsley et al., 2006). To alleviate this pain, secondary interventions such as hardware revision, arthroplasty, corrective osteotomy and in many cases hardware removal may be necessary (Meier et al., 2006; Benegas et al., 1987). Hence it is important to understand the advantages and limitations of such treatments.

To prevent the occurrence of varus collapse, we analyzed the fractured specimens and two important factors were identified which alone or together influenced the fixation of the proximal humeral fractures. They were: 1) calcar comminution of the medial cortex; and 2) poor use of calcar fixation. We presently hypothesized that the lack of medial cortical contact critically destabilize proximal humerus fractures but with calcar fixation, the medial stability can be restored thus preventing varus collapse.

1.2 Rotator Cuff Repairs

Critical to the success of surgery is the repair stability allowing early range of motion without loss of reduction. Complex humeral head fractures, in particular, those with displaced tuberosities, are frequently associated with a longitudinal tear of the rotator cuff. Numerous studies show that functional outcome of the fixation of proximal humeral fractures well correlate with rotator cuff repair integrity (Porcellini et al., 2006; Wilmanns et al., 2002). The disruption of the rotator cuff can directly affect the loads sustained on the glenohumeral joint (Parsons et al., 2002). If not reduced sufficiently, this may result in a tendinous gap, an uncovered humeral head, and alterations of the rotator

cuff. Thus there is a need for a careful rotator cuff repair in order to optimize treatment results.

The rotator cuff tears can be surgically treated with the help of arthroscopic stitches. Many techniques have been described to improve the biomechanical properties of arthroscopic stitches (MacGillivray et al., 2004; Scheibel et al., 2003; Sileo et al., 2007). However, these stitch configurations may involve additional materials or additional steps that can increase the cost, complexity, and length of surgery. The current stitches frequently used in arthroscopic surgery include the simple, mattress, a combination of the two which is termed a MAssive Cuff stitch (MAC) (MacGillivray et al., 2004) and Modified Mason-Allen (MMA) stitch (Ma, et al., 2004).

It is widely accepted that the weakest aspect of the repair construct remains the tissue-suture interface (Burkhart et al., 1997; Cummins et al., 2003). The importance of repair healing has been demonstrated with improved outcomes in successful repairs compared to failed repairs (Gazielly et al., 1994). This further emphasizes the need to identify techniques to improve the strength of repairs, open or arthroscopic, in an attempt to improve the rates of healing.

The lasso loop stitch that was recently designed to improve tissue grip, is a technically simple arthroscopic stitch that does not involve additional implants and frequently reduces the number of implants used in shoulder arthroscopy (Lafosse et al., 2006). Similar to the MMA stitch, the lasso loop can be easily placed arthroscopically and

similar to the MAC stitch, the lasso loop limits suture pull out through the tendon by grasping the repaired tissue. While this stitch technique has been used with good clinical results, it has not yet undergone formal biomechanical testing (Lafosse et al., 2007).

Thus in the second part of this study, biomechanical evaluation of the lasso loop stitch in comparison with other stitches was carried out. Also the impact of the tissue penetrator geometry and the tissue bite size has upon tissue holding strength characteristics rotator cuff repair stitches.

CHAPTER 2

LITERATURE REVIEW

2.1 Shoulder Anatomy

The shoulder joint (Fig. 1) is made up of three major bones; namely, the humerus (upper arm bone), the scapula (shoulder blade), and the clavicle (collarbone) as well as associated muscles, ligaments and tendons. The humerus is the largest and longest bone of the upper extremity. Some of the important anatomical features of the humerus are the humeral head (half-spheroid articulating surface in proximal part), greater tubercle, intertubercular (bicipital) groove, lesser tubercle, surgical neck and the humeral shaft. The greater tubercle has 3 facets into which the tendons of the supraspinatus, infraspinatus, and teres minor join. The lesser tubercle is the site of insertion of the subscapularis, completing the rotator cuff.

The second major bone, the scapula is a large, thin, triangular bone lying on the posterolateral aspect of the thorax, which serves mainly as a site of muscle attachment. The superior process, or spine, separates the supraspinatus muscle from the infraspinatus and extends to form the base of the acromion. The spine functions as part of the insertion of the trapezius muscle, as well as the origin of the posterior deltoid muscle (Terry et al, 2000). The acromion forms a portion of the roof of the space for the rotator cuff, and variations in acromial shape can affect contact and wear on the rotator cuff (Terry et al,

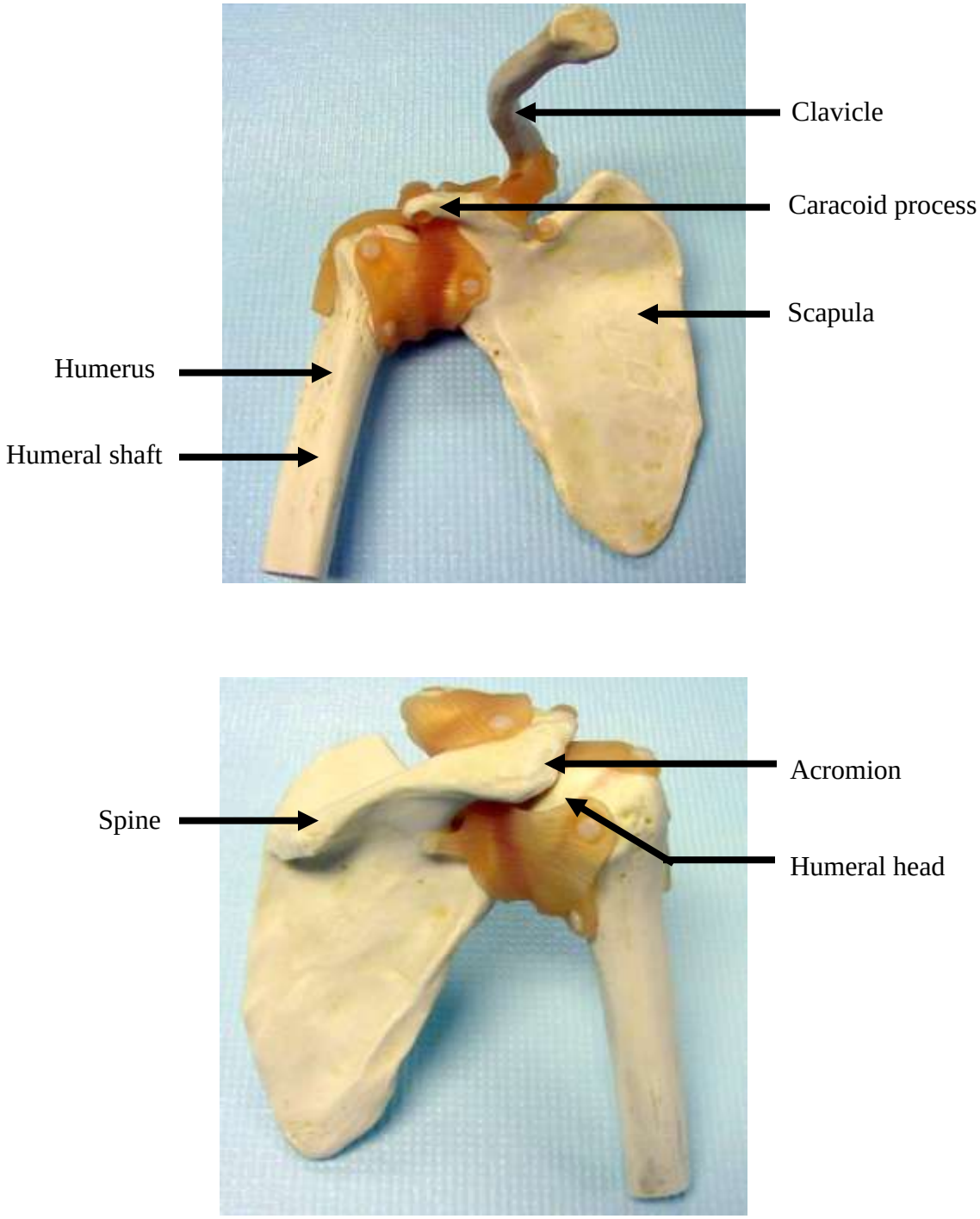

Figure 1: Anterior (top) and posterior (bottom) view of shoulder joint.

2000). The coracoid process projects anteriorly and forms the upper border of the head of the scapula.

The final major bone in the shoulder joint is the clavicle and it serves as the sole bony strut connecting the trunk to the shoulder girdle. This specific arrangement of the clavicle keeps the humerus away from the thorax so that the arm has maximum range of movement. The clavicle also serves as a site for muscle attachments. In addition to this, it acts as a barrier to protect underlying neurovascular structures, and a strut to stabilize the shoulder complex and prevent it from displacing medially with activation of the pectoralis and other axiohumeral muscles. Additionally, the clavicle prevents inferior migration of the shoulder girdle (Craig, 1997).

.

2.2. Joint Articulations

The articulations between the bones of the shoulder make up the shoulder joints. Its large range of motion is made possible by the interplay of four joints; namely, glenohumeral joint, sternoclavicular-joint, acromioclavicular-joint and scapulothoracic joint (Jansen et al, 2001).

The glenohumeral joint is the main joint of the shoulder. It is a ball-and-socket joint that allows the movement like flexion, extension, abduction and adduction. It is formed by the articulation between the head of the humerus and the lateral scapula. The "ball" of the joint is the rounded, medial anterior surface of the humerus i.e. the humeral head and the "socket" is formed by the glenoid fossa, which is the dish-shaped portion of the latter

scapula. The surface area of the glenoid socket is approximately one-third that of the surface area of the humeral head (Kelkar et al, 2001). Thus, the humeral head does not fit perfectly within the glenoid socket. This size discrepancy creates a situation where the two bones do not securely fit together without the help of other physical structures. Thus this joint is dependent primarily on soft tissues for stability. A combination of muscles, capsules and ligmentous forces is necessary for the normal motion to occur (Kelkar et al, 2001).

The labrum is a rim of fibrocartilage that lies directly between the humeral head and the glenoid provides a smooth surface that allows for the humeral head to rotate with minimal friction, thus cushioning both the humerus and the scapula. The joint capsule is a thin sheet of fibers that surrounds this joint. The capsule of the shoulder is attached along the outside ring of the genoid cavity and the anatomical neck of the humerus. This allows a wide range of motion yet provides stability. Also it is lined by a thin, smooth synovial membrane which secretes the synovial fluid. The conformity of the glenoid and the humeral surfaces along with the synovial fluid present, passively stabilize the glenohumeral articulation.

The main muscles that associated with the glenohumeral joint are the supraspinatus, subscapularis, infraspinatus, and teres minor (rotator cuff). All four of these muscles connect the scapula to the humerus. In addition to the labrum, capsule and the rotator cuff muscles, six other ligament help with the stabilization and movement of this joint (Kwak et al, 1998).

The acromioclavicular joint formed between the clavicle and the scapula is a gliding joint which gives the ability to raise the arm above the head. This joint helps with movement of the scapula, thus resulting in a greater degree of arm rotation (Terry et al, 2000). Also, this joint allows the transmission of force from the upper arm to the rest of the skeleton. Like the glenohumeral joint this joint requires the action of various ligaments and muscles for its stability. The muscle sets which are associated with this joint are the trapezius muscle and the deltoid.

The sternoclavicular articulation forms the only skeletal articulation between the upper extremity and the thorax. This is a sellar (saddle) joint formed by the medial end of the clavicle, the clavicular notch, and the cartilage of the first rib. Because of the size disparity between the large bulbous end of the clavicle and the smaller articular surface of the sternum, stability is provided by the surrounding ligamentous structures (Terry et al, 2000, Klein et al, 1995).

The scapulothoracic articulation is the space between the convex surface of the thoracic cage and the concave surface of the anterior scapula. It is occupied by neurovascular, muscular, and bursal structures that allow a relatively smooth motion of the scapula on the underlying thorax. With the scapula serving as the bony foundation of the shoulder girdle, this joint allows increased shoulder movement beyond the 120^0 (Terry et al, 2000). Seventeen muscles attach to or originate from the scapula and function to stabilize this joint and provide the motion.

2.3 Fracture Patterns and Classification

Proximal humerus fractures represent a common condition. It is the third most common type of fracture seen in elderly patients and account for 10 percent of all fractures. Also studies have predicted a three-fold increase over the next three decades (Baron et al., 1996, Kannus et al., 2000). Management of these injuries is complicated by several factors because of the complex anatomy. Some fracture patterns may compromise the vascularity of the humeral head, while other patterns are complex and are difficult to understand according to imaging studies. Also, bone quality plays a key role and the overall geometry of the proximal humerus and may be difficult to reestablish when humeral head replacement becomes necessary (Diederichs et al., 2006).

The basic anatomic elements of proximal humerus fracture classification were outlined by Neer (Neer, 2002). The Neer system classifies the fractures based on displacement of each of these segments and in addition, considers the presence of associated dislocation, impaction, or division of the head. The new classification was called the "four segment classification" which is based on the "One centimeter or forty-five degrees" displacement criteria. The limits of 1.0-cm displacement or 45° angulation were arbitrarily set as the displacement criteria for classification.

One-part fractures (minimal displacement): Eight out of ten proximal humeral fractures are of this type. This category includes all fractures of the proximal humerus, regardless of the level or number of fracture lines, in which no segment is displaced more than 1 cm or angulated more than 45°.

Two-part articular segment displacement (anatomic neck): This is characterized by isolated displacement of the articular segment at the anatomic neck level, without displacement of the tuberosities. The undisplaced tuberosities prevent the articular surface from being displaced in valgus.

Two-part shaft displacement (surgical neck): This type of fracture occurs in patients of all ages. There may be hairline, undisplaced fissure fractures proximally in the tuberosities, but they and the articular segment are held in neutral rotation by the rotator cuff muscles. There are 3 clinical types, each with special treatment considerations.
Impacted: For the impacted type, there is more than 45° angulation and the apex is usually anterior. The periosteum is intact on the side opposite the apex.
Unimpacted: In this, the pectoralis major act to displace the shaft anteromedially and the head tends to remain in neutral rotation.
Comminuted: For the comminuted type, fragmentation of the upper shaft is present and the pectoralis major may retract a large fragment the head and tuberosities are held in neutral rotation by the rotator cuff.

Two-part greater tuberosity displacement: Two-part greater tuberosity displacement is usually seen with an anterior dislocation that has reduced after relocation of the head. The segment is usually fragmented and one or all of its three facets for the rotator cuff attachments are retracted, causing a tear in the rotator cuff and covering a portion of the articular surface (Neer, 2002).

Two-part lesser tuberosity displacement: As the name indicates, in this type the lesser tuberosity is displaced with respect to the humeral head.

Three-part displacements: In 3-part displacements one of the tuberosity is displaced and there is a displaced unimpacted surgical neck component that allows the head to be rotated by the other non-displaced tuberosity. When the greater tuberosity is displaced, the head is rotated internally. When the lesser tuberosity is displaced, the head is rotated externally (Sanchez, 2006).

Four-part fractures: In a true 4-part fracture (lateral fracture-dislocation), the articular segment is displaced out of contact with the glenoid (i.e., dislocated), detached from the shaft and both tuberosities, and detached from its blood supply. The exception is the valgus-impacted type of 4-part fracture which is a less-displaced, borderline lesion.

This classification was intended to help understand the pathoanatomy of different fracture patterns, which may be difficult to infer based on radiographs alone. Understanding proximal humerus fractures is complicated by variation in fracture patterns and difficulties interpreting two-dimensional radiographs in different positions of the arm. The increased use of computed tomography with three-dimensional reconstruction represents a major advance in the evaluation and treatment of proximal humerus fractures.

2.4 Fracture Fixation

Most proximal humerus fractures occur in patients with osteopenia (Anderson et al., 1999). Due to this, there is a high degree of comminution which increases the magnitude of cancellous defects, and the potential for fixation failure and fracture redisplacement in an impact event. Internal fixation of proximal humerus fractures can be improved by increased awareness of regions within the proximal humerus with increased bone mineral density (Diederichs et al. 2006) and also by the use of modern low-profile fixed-angle devices designed for fixation in osteopenic bone (Sanchez, 2006). Bone quality and mineral density are different in different regions of the proximal humerus (Diederichs et al, 2006). Knowledge of areas with better bone quality may be used to achieve stronger implant fixation and decrease the risk of hardware failure.

Hepp et al. (2003) used 24 fresh human cadaveric humeri to determine the histomorphometric and bone strength distribution in the anterior, posterior, medial, lateral, and central regions of four different proximal to distal levels of the humeral head. The best bone was found in the medial and dorsal aspects of the head, and bone quality decreased from proximal to distal (Hepp et al., 2003). Better bone mineral density was found in the proximal compared to the distal half of the humeral head. The posterior aspect of the greater tuberosity had higher trabecular BMD compared to its anterior aspect; greater tuberosity cortical BMD was higher in the middle aspect proximally and the anterior aspect distally (Tingart et al., 2003).

Internal fixation of proximal humerus fractures can be improved by the use of specifically designed devices. There are numerous procedures available for fixation like semi-rigid (percutaneous k-wiring, screw fixation, tension band wiring) and rigid (conventional plates and screws, intramedullary nailing) means (Charalambous et al., 2007; Florian et al., 2003).

Presently most proximal humerus fractures are treated using locking plates which are anatomically contoured plates that allow placement of multiple locked screws in the humeral head (Egol et al., 2004). Ideally, the devices used for proximal locking should provide fixed-angle fixation. It was found that locking plates stabilized the fracture to union in a satisfactory position, for a majority of proximal humerus fractures (Charalambous et al., 2007). Also Sara et al., (2006), found that a locking compression plate for the proximal part of the humerus demonstrated superior biomechanical characteristics compared with the proximal humeral intramedullary nail when tested in both cyclic varus bending and torsion.

One particular design in locking plates is called the Locking Compression Proximal Humerus Locking Plate (LCP-PHLP, Synthes, Paoli, PA). Its shape is anatomical, conforming to the proximal humerus (Fig. 2). In the humeral head component of the plate, there are five pairs of combi-holes (A, B, C, D and E holes) through which locking screws are inserted in multiple directions into the humeral head (Fig. 2). The placement of these holes is designed in such a way that they not only provide flexibility in screw placement, but also permits multiple points of fixation to support the humeral head which

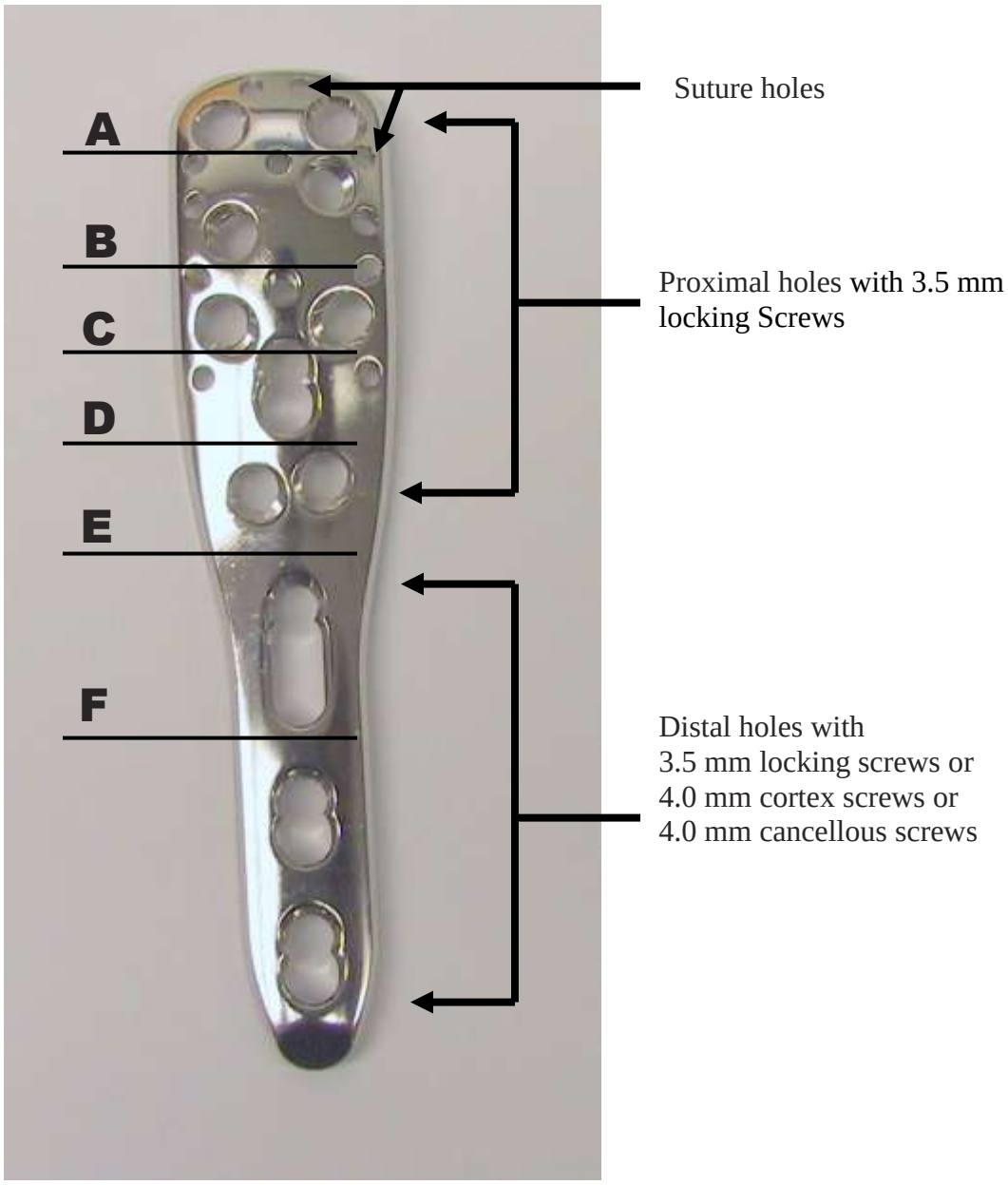

Figure 2: Proximal Humeral Locking Plate (PHLP)

is essential as it was shown by Liew et al. (2000) that the bone with the greatest purchase is center-center subchondral position in the humeral head. In the shaft component of the implant combi-holes provide the option of locking or non-locking screws to be inserted. Smaller holes allow the passage of sutures or wires to help reattachment of the greater and lesser tuberosities. The implant comes in short and long sizes with three and five shaft combi-holes, respectively.

Despite the added strength provided by the locking plate over conventional fixation, hardware failure with collapse of the fracture into varus is noticed in many cases (Plecko et al., 2005). Also it has been noticed that numerous secondary interventions ranging from hardware removal to hardware revision to arthroplasty have been necessary at the expense of added morbidity to the patient.

The concept of "calcar restoration" of the proximal humerus was introduced by Gardner et al. (2007) in which they found that surgical reduction of the calcar significantly reduced the rate of varus collapse. Even though clinical evidence supports that appropriate reduction at the time of surgery, with near anatomical restoration of the neck-shaft angle, decreased the rates of varus collapse (Weinstein et al, 2007) no such relation ship between the calcar restoration and the varus collapse have been established.

2.5 Rotator Cuff Tears

The rotator cuff is a group of muscles consisting of the subscapularis, supraspinatus, infraspinatus, and teres minor, which act as a dynamic stabilizing mechanism for the

humeral head. Experimental studies have demonstrated that the rotator cuff serves two principle functions at the glenohumeral joint: (1) generation of torque which is important for rotation of the humerus on the glenoid; and (2) compression of the humeral head into the glenoid concavity. This latter function of glenoid compression compensates for the lack of inherent bony stability at the glenohumeral joint, thus serving as the primary stabilizing mechanism for this minimally constrained articulation during the functional range of motion (Karduna et al., 1996; Warner et al, 1998).

Rotator cuff tears are very common during sports activities. Also complex humeral head fractures are frequently associated with a longitudinal tear of the rotator cuff. Tearing of the rotator cuff not only results in shoulder pain but also lead to altered biomechanics of the shoulder. Rotator cuff tear often displaces the greater tuberosity superiorly and posteriorly, while the lesser tuberosity is frequently displaced inferiorly and medially by muscular forces. Thus if not reduced sufficiently, this may result in a tendinous gap, an uncovered humeral head, and alterations of the rotator cuff.

Although many tears can be treated conservatively, rotator cuff surgery is considered when non-operative treatment fails. Thus arthroscopic repair has become an established surgical technique for the treatment of rotator cuff tears. Rotator cuff repair can only be considered as long as the quality of the torn rotator cuff is still sufficient. Despite continual improvement in surgical techniques and instrumentation, re-tear of the tendons does occur in many patients (Mansat et al., 1997).

The repaired rotator cuff has several potential points of weakness: the tendon–suture interface, the suture itself, the suture–eyelet interface, and the bone–anchor interface. Early rotator cuff failures were observed to be caused by either failure of the knot at the suture anchor; however, the majority of the failures occur when the suture pulls out through the tendon (Cummins et al., 2003). Thus the weakest link has been shown to be the suture-tendon interface (Gerber et al., 1999; Rossouw et al., 1997). In addition, weak initial fixation with stretching of the repair can lead to gap formation between the repaired tendon and the osseous insertion and subsequently to poor tendon-to-bone healing (Burkhart et al., 1998). Thus one needs to identify techniques to not only improve the strength of repairs, but also in an attempt to improve the rates of healing.

2.6 Arthroscopic Repair Techniques

Many suture techniques have been described in the literature to improve the biomechanical properties of arthroscopic stitches (Gerber et al., 1999, Scheibel et al., 2003). However, some of the stitch configuration involves additional surgical tools and methods for arthroscopic placement thus leading to increase in cost, complexity, and length of surgery. The current suture techniques frequently used in arthroscopic surgery include the simple stitch, the horizontal mattress stitch, the massive cuff stitch (MAC) which is the combination of both simple and mattress. Ma et al., (2004) showed that both simple and mattress stitch had comparable biomechanical properties, while the MAC stitch was stronger than simple or mattress stitches when tested in sheep tendons.

The modified Mason-Allen (MMA) stitch is another stitch which is commonly used for rotator cuff tears. However, this stitch is used in open repairs as this stitch is quite difficult to perform arthroscopically. This stitch has been proven to be biomechanically stronger than simple or mattress stitches when tested in sheep tendons in vitro (Ma et al., 2004). Also the MMA stitch has long been the gold standard against which other suture configurations have been compared (Schneeberger et al., 2002).

The lasso loop (LL) stitch is a technically simple arthroscopic stitch that does not involve additional implants and frequently reduces the number of implants used in shoulder arthroscopy (Lafosse et al., 2006). In the LL stitch, "the mid-portion of a suture is passed through the tissue creating a loop of suture that allows the free suture end to be grasped and brought through the loop creating a self-cinching stitch" (Fig. 3). The LL technique is versatile and has been used in arthroscopic bicep tenodesis, as well as in rotator cuff repairs (Lafosse et al., 2006).

Lasso loop stitch similar to the MAC stitch can be easily placed arthroscopically and limits suture pull out through the tendon by grasping the repaired tissue. However, in contrast to the MAC, the LL can be placed with one (simple stitch) or two (mattress stitch) passes through the tissue as opposed to three passes. Also, unlike the MAC stitch, the lasso loop does not require additional suture to be placed, further simplifying and expediting the repair. While LL stitch technique has been used with good clinical results (Lafosse et al., 2006), it has not yet undergone formal biomechanical testing.

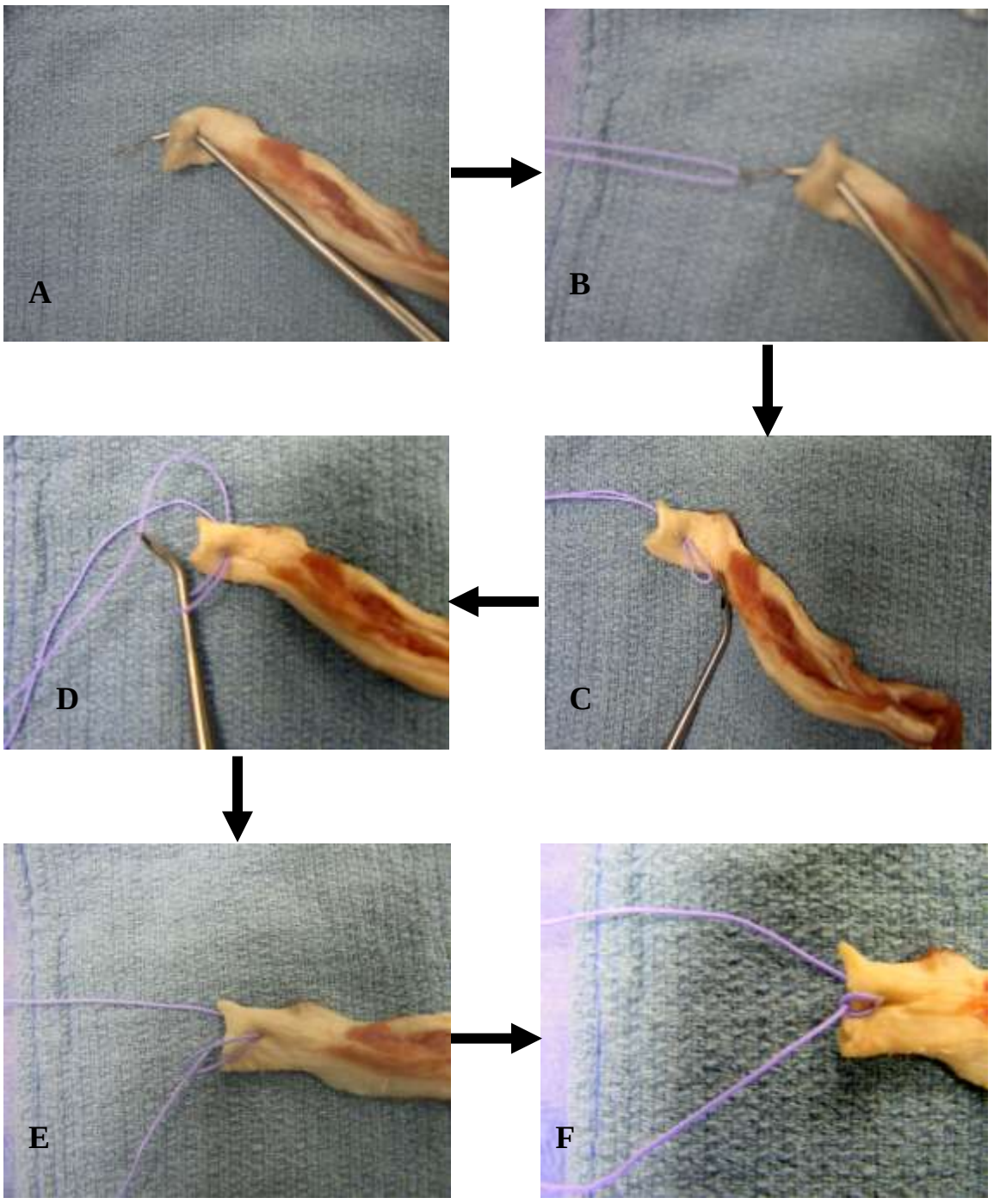

Figure 3: Figure showing the process by which the lasso loop is placed (A through F).

The strength of the tendon-suture interface does not just depend on the type of suture placed, but may also depend on the type of tissue penetrator used for placing the sutures. Numerous studies have examined the types of suture/ suture anchors used with very little emphasis on the device for suture passage (Cummins et al., 2003; Burkhart et al., 2002). Numerous arthroscopic devices with varied size and shape are used in rotator cuff repairs. Differences in the tissue penetrating geometries may affect stitch strength. Hence a proper understanding of the instrument used for the placing the suture is also needed for improving the healing rates.

Another parameter that may influence in the tendon suture strength is the bite size. Larger tissue purchases have been demonstrated to improve footprint coverage, but we are presently unaware of any relationship between bite size and stitch strength. Hence evaluating the influence of bite site is also needed for a proper tendon repair.

CHAPTER 3

PURPOSE

As mentioned earlier, the PHLP is designed to allow for five pairs of locking screws to be placed in the humeral head. The most distal locking screw options in the humeral head (the E-hole screws) are positioned and angled such that they are placed along the most inferior aspect of the surgical neck and humeral head and, in many cases, cross the fracture site. Nowhere in the surgical technical guide or in the orthopaedic literature has the relative importance of one row of locking screws over another been emphasized in stabilizing the proximal humerus fractures.

Also, there is a need to assess the role of calcar comminution and the importance of calcar stabilization in the use of proximal humerus locking plates as medial fracture comminution has not been well studied and varus collapse continues to be a clinical problem.

Hence we hypothesized that:

1. Calcar comminution is a determinant of fracture fixation and fracture stability; and
2. Greater stability and increased resistance to varus deformity is obtained through use of long locking E-hole screws which cross the inferior surgical neck and penetrate the humeral head.

The second part of this study evaluates the biomechanical properties of the lasso loop stitch in comparison to other common stitches used in shoulder surgery: namely simple, mattress, MMA and MAC stitches. Also this study evaluates the impact that the size of the tissue penetrator has upon stitch holding strength. To our knowledge, very limited insight has been found in the literature that addresses the stitch strength based on the size of tissue penetration. Finally this study also investigates the effect of tissue bite size through the tendon has upon the holding strength of commonly used stitches. Even though larger tissue purchases have been demonstrated to improve footprint coverage, we are presently unaware of any relationship between bite size and stitch strength placed for the rotator cuff repair.

Thus we hypothesized that:

a) the lasso loop stitch will have similar properties to the MAC and MMA stitches and will have better biomechanical properties when compared with simple and the mattress stitch.
b) bigger tissue penetrator will have lower load to failure values than the smaller diameter tissue penetrator.
c) bigger bite size will have higher suture holding strength than smaller bite size.

CHAPTER 4

MATERIAL AND METHODS

4.1 Proximal Humerus Fracture Fixation

4.1.1 Specimen preparation

Following IRB approval, eleven pairs of fresh frozen humeri harvested from fresh frozen cadavers were used for the study. The mean age of the cadavers was 63.3 years, with a range of 38 to 86 years. All cadavers were screened for cause of death, and their humeri were grossly inspected for deformity. The humeri were stripped of their entire adherent soft tissues and dual energy x-ray absorptiometry (DEXA) scans of each humerus were obtained to provide a measure of bone mineral density within the humeral head. Also each specimen was analyzed with fluoroscopy to ensure there were no pre-existing osseous defects prior to testing. Finally, after removing the distal humeral condyles the humeri were stored as pairs in sealed bags at -20°C.

4.1.2 Fracture simulation and fixation

In order to test the hypothesis, four different fractures construct was created. In all the specimens, a simple, reproducible, non-comminuted, 10° oblique, three-part surgical neck fracture which has been previously described in the literature (Neer CS, 1970) was simulated using a band saw by an experienced surgeon. Additionally in five of the humeri pairs, a 1-cm bone resection across the calcar region was made to mirror the medial

comminution. Thus we created two fracture groups, namely; medial comminution and non-comminution group.

Once the fracture has been simulated, all the specimens were fixed with the help of Proximal Humerus Locking Plate. In every construct, all the seven proximal locking screws (the A, B, C, and D holes) were filled. However within each matched pair of humeri (left Vs right), one received long E-hole locking screws (40 mm) which crosses the fracture site and penetrates into the humeral head thus providing good calcar support while the other had short E-hole screws (25 mm) which did not cross the fracture site thus did not have a calcar support (Fig. 4). Thus, we established four different conditions: 1) Medial comminuted with short calcar screws (MCS) and 2) Medial comminuted with long calcar screws (MCL) 3) Non-comminuted with short calcar screws (NCL); and 4) Non-comminuted with long calcar screws (NCS) (Fig. 5, 6).

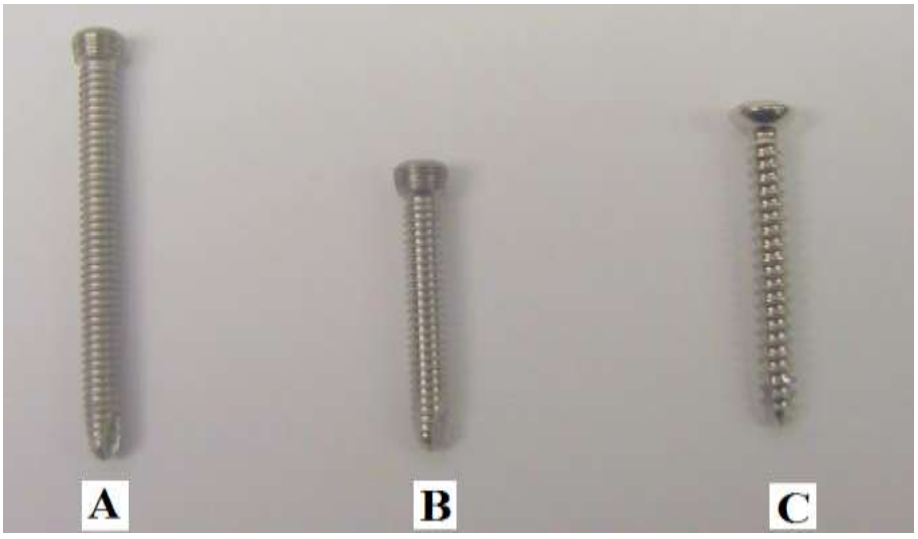

Figure 4: Types of screws used in PHLP construct.
A) long (40 mm) calcar (E-hole) screws B) short (25 mm) calcar screws
C) non locking humeral shaft screws.

4.1.3 Testing Protocol

Mechanical testing was performed using a previously established method by Koval et al. (1996) in which the distal humerus was potted in polymethyl methacrylate (PMMA; CG America Inc., Chicago, IL) using an aluminum cup. This is then placed inside the steel tubing oriented at 20° and welded to the base plate (Fig. 7). This model closely reproduced the longitudinal direction of force encountered at the geometrical center of the humeral head seen with early active abduction. The steel tubing contained four lateral screws which aided in holding the aluminum cup potted with the humerus at a fixed position. Vertical compressive loads were then applied to the superior aspect of the humeral head 0.5-cm medial from the lateral groove, using a 2-cm diameter cupped cylinder. The constructs were continuously loaded to failure at a rate of 10 cm/min by an 858 Mini Bionix uniaxial servohydraulic Materials Testing System (MTS Systems Corp., Eden Prairie, MN, USA).

Actuator force and displacement were recorded using the MTS TestStar software. Failure was defined as either marked decrease or discontinuity in the load-displacement curve or expansion of the simulated fracture line along the medial cortex in case of non-comminuted fractures and completion of varus angulation with closure of the medial cortical defect in case of medial comminuted fractures.

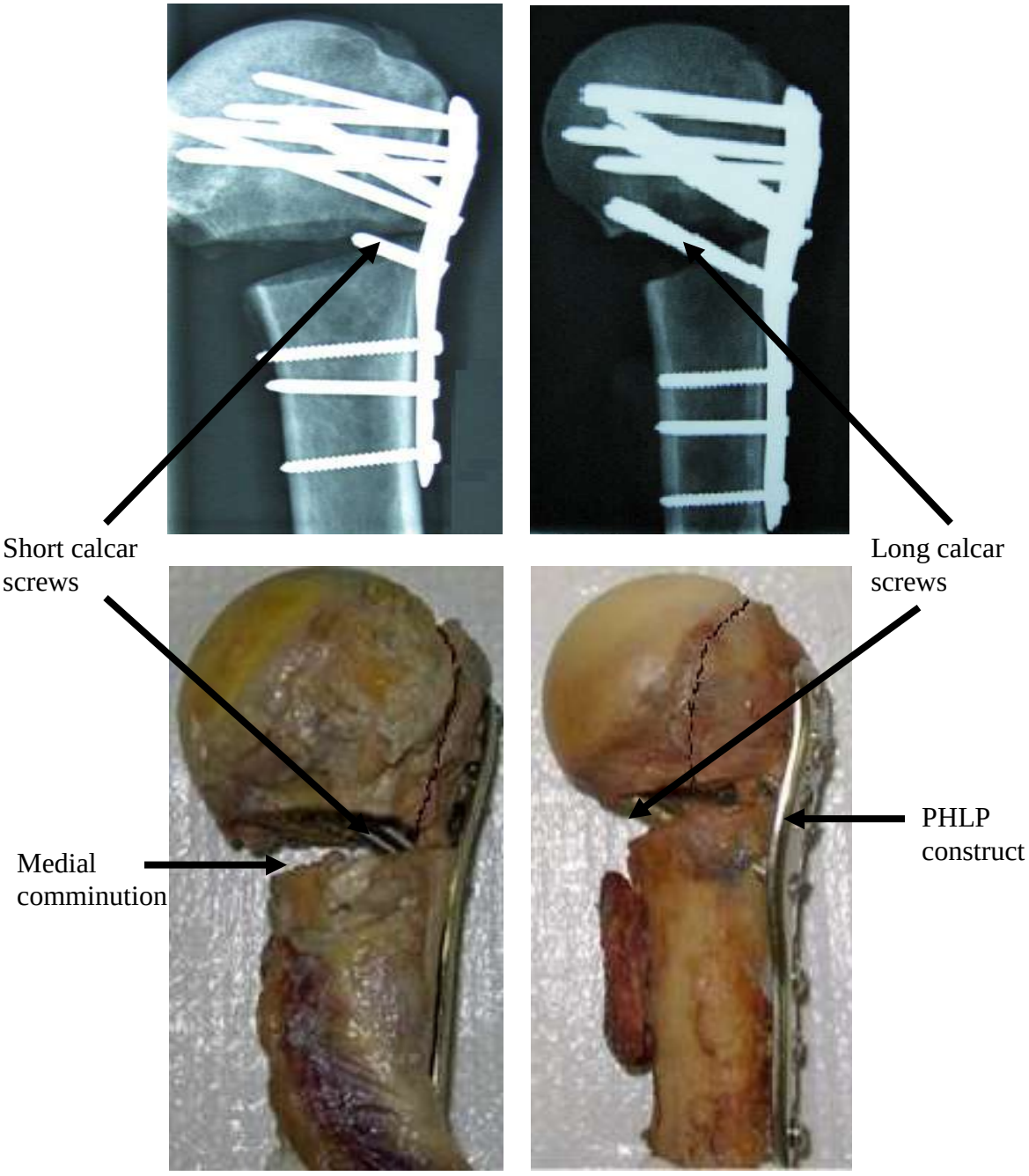

Figure 5: Correlation between the radiographs and the fracture constructs for medial comminutied specimens.

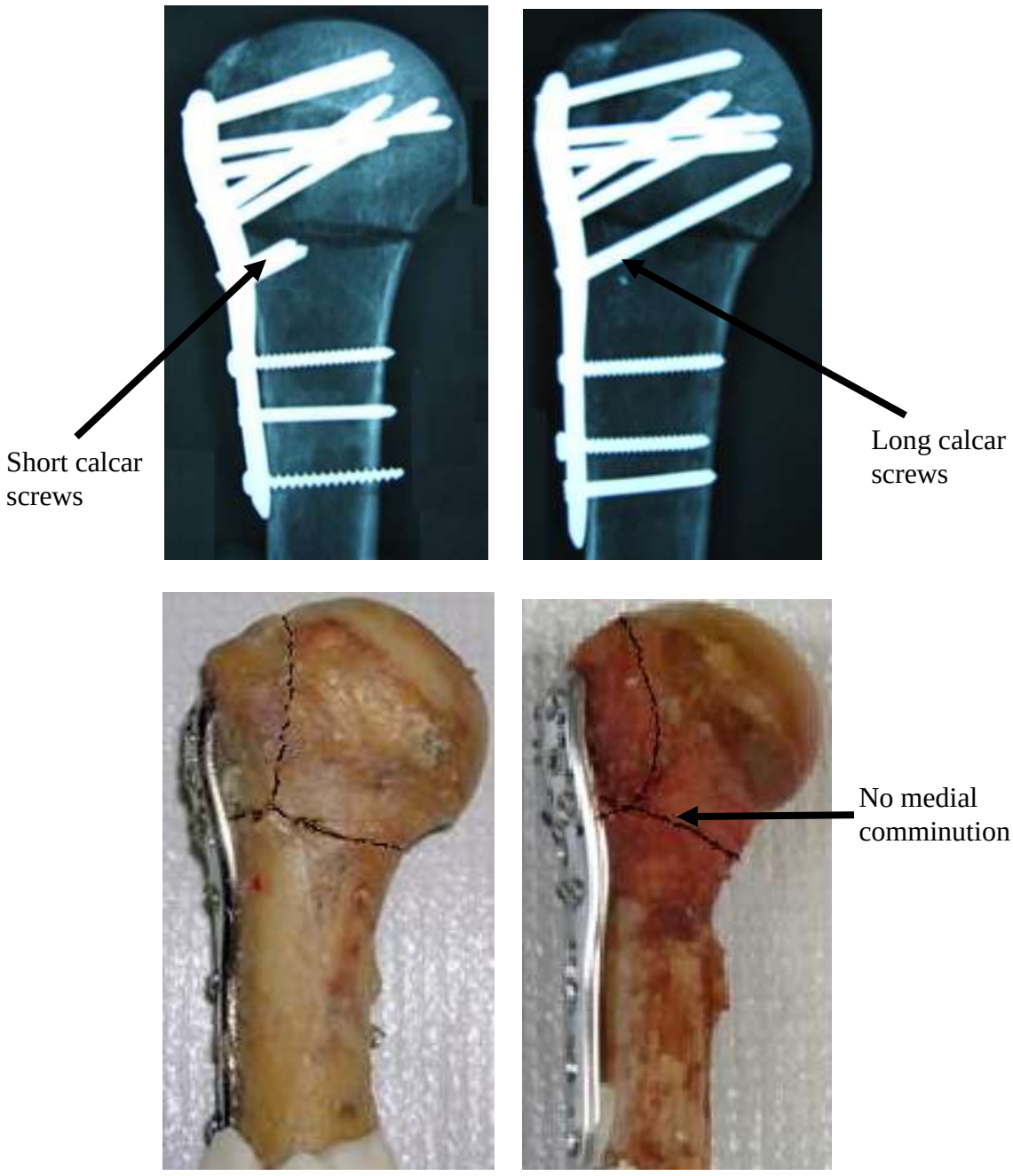

Figure 6: Correlation between the radiographs and the fracture constructs for non-comminuted specimens.

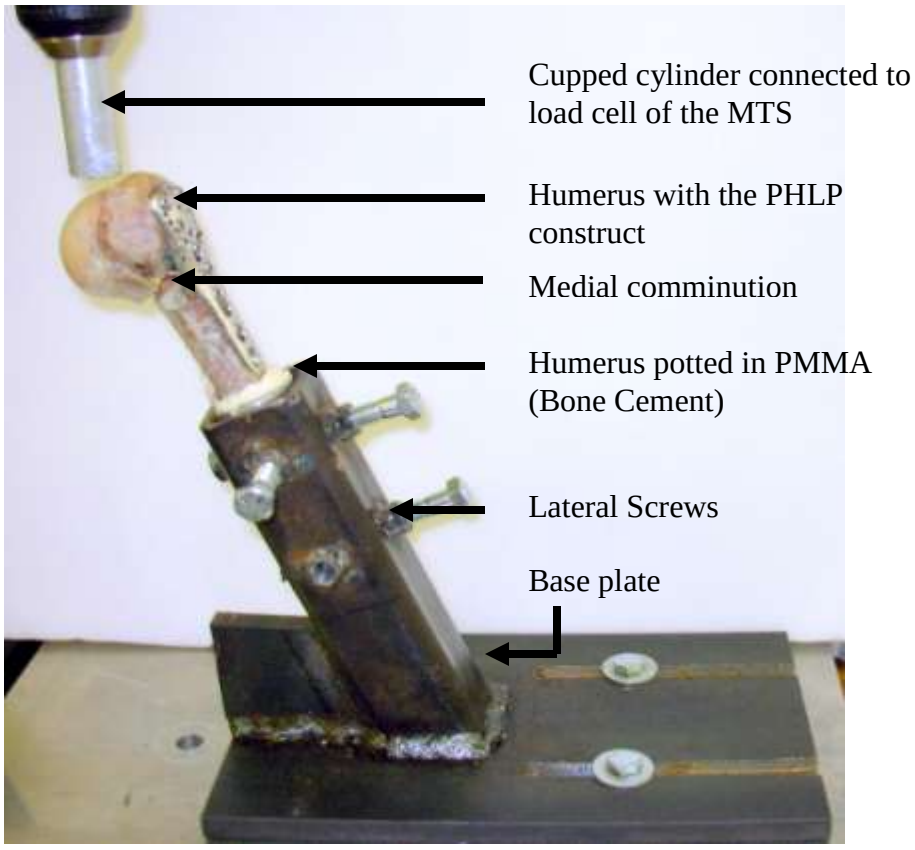

Figure 7: Jig used for the biomechanical Testing

4.1.4 Data and statistical analysis

Following testing, the actuator load and displacement data was transferred to Excel software (Microsoft Corporation, Seattle, WA) to create load-displacement curves. From the load-displacement curves obtained for each construct, values for stiffness, load to failure, displacement at failure, and energy to failure were determined (Fig 8, 9). Each test was also recorded with a digital camera so as to capture the different modes of failure for the constructs.

Stiffness was calculated as the slope of the linear portion (point until which the deviation increases) of the load-displacement graph. The load to failure was obtained by comparing the load-displacement graphs with the respective videos taken during the trail (Fig. 10, 11). Energy to failure was taken as the area under the curve until the point of failure. Displacement corresponding to failure load was considered as the displacement at failure. Two-way Analysis of Variance (ANOVA) was used to evaluate the differences in measurements due to comminution, and the type of screw used for fixation.

Also a multivariate, random intercept regression model was fitted for each outcome using SAS version 8.02 (SAS Institute, Cary, NC). This technique properly accounts for the paired nature of the specimens and quantifies the degree of correlation between matched pairs. Various models were explored considering Bone Mineral Density (BMD) as a linear or categorical variable, and all interactions (fracture type by screw length, fracture type by BMD, screw length by BMD) were examined with the alpha level of significance set at $p < 0.05$.

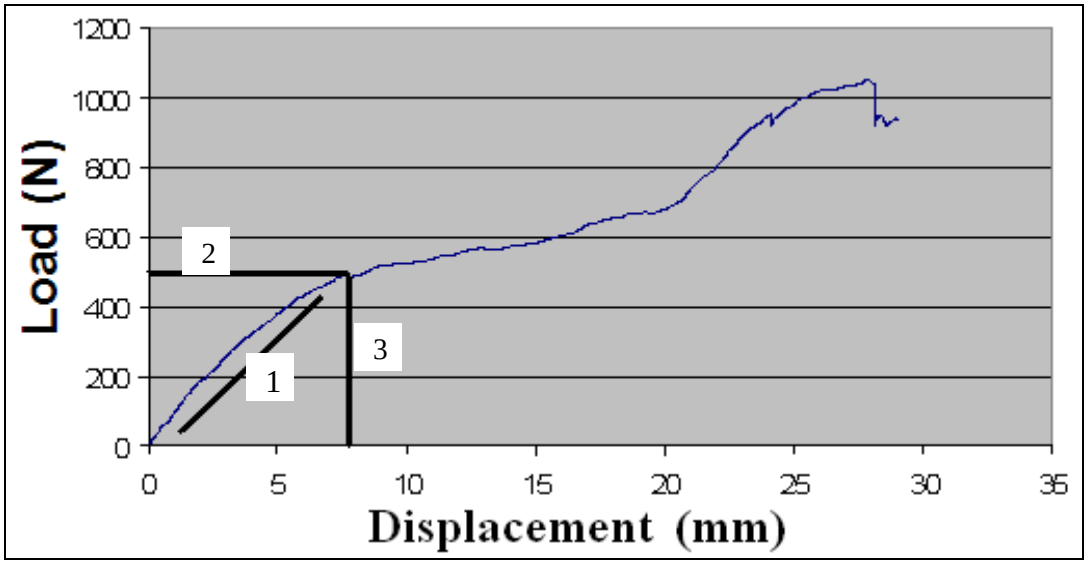

Figure 8: Load-displacement graph for medial comminuted specimen
1) stiffness, 2) load to failure and 3) displacement at failure

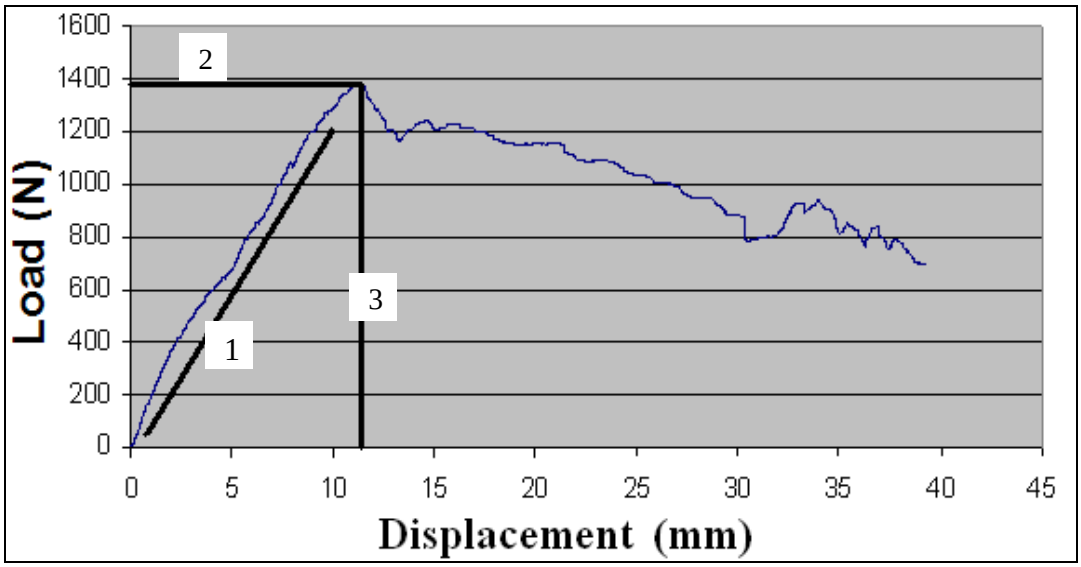

Figure 9: Load-displacement graph for non-comminuted specimen
1) stiffness, 2) load to failure and 3) displacement at failure

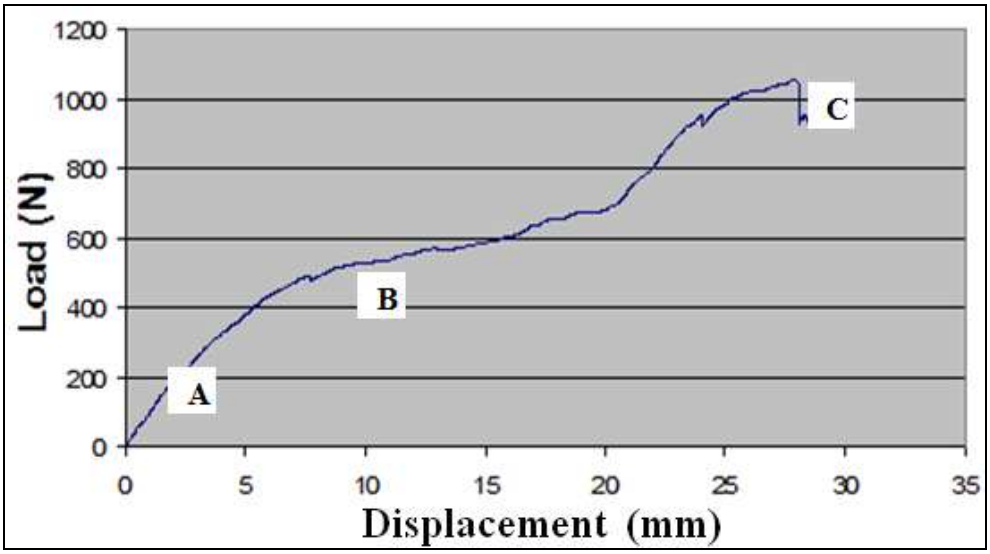

A: Start of experiment

B: Completion of varus angulation

C: Screw pullout.

Figure 10: Correlation between the video taken with the load-displacement graph for medial comminuted trail.

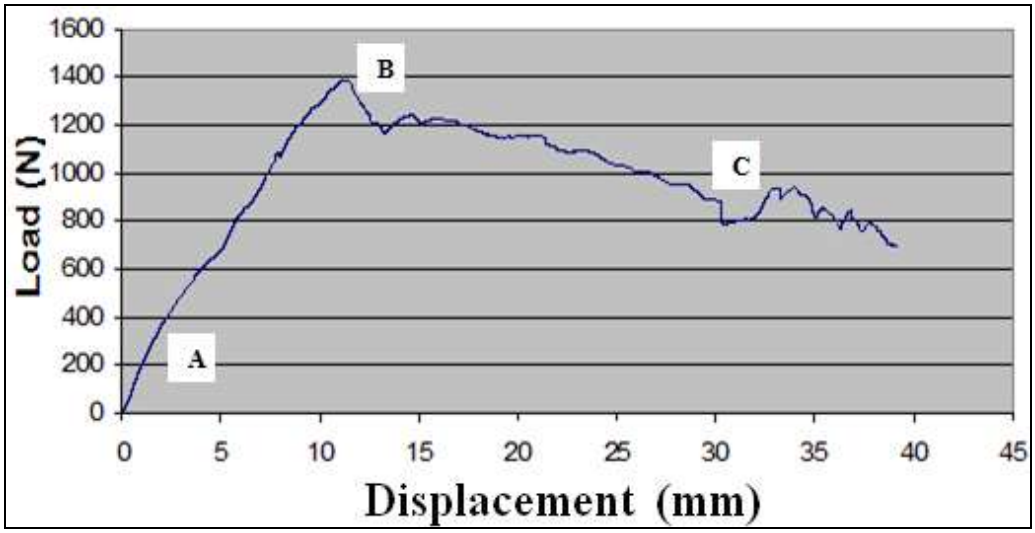

A: Start of experiment

B: Initiation of failure

C: Screw pullout.

Figure 11: Correlation between the video taken with the load-displacement graph for non-comminuted trail.

4.2 Evaluation of Rotator Cuff Repair Techniques

4.2.1 Specimen Preparation

Thirty-one sheep shoulder pair was harvested from which the infraspinatus tendon was dissected free from the surrounding muscles and any bone attachments. Paired cadaveric sheep shoulders were chosen based upon prior studies demonstrating similarities in the size, shape, and microstructure of sheep cuff tendons and human cuff tendons (Gerber et al., 1994). Each tendon was cut approximately 5-cm in length and was split in half longitudinally to yield four tendon specimens from each pair of shoulders (Fig. 12). Thus, a total of 124 tendon grafts were obtained. All tendon grafts was visually inspected for any gross abnormalities or defects and none were excluded from testing.

4.2.2 Group Allocation

These 124 tendon grafts was divided among three groups:

Group 1: Forty tendon grafts was used for the evaluating the lasso loop stitch. These 40 grafts were equally divided among the five stitches: namely simple, mattress, MMA, MAC and lasso loop stitch (Fig. 13). Thus we obtained a sample size of eight for each group. The suture in each graft was placed 0.5-cm from the distal tendon end by an experienced surgeon. All suture used in this study was #2 Orthocord, which is a braided ultrastrong permanent suture (Depuy Mitek, Raynham, MA). The stitches was placed using the Clever Hook (DePuy Mitek, Raynham, MA), tissue penetrator.

`

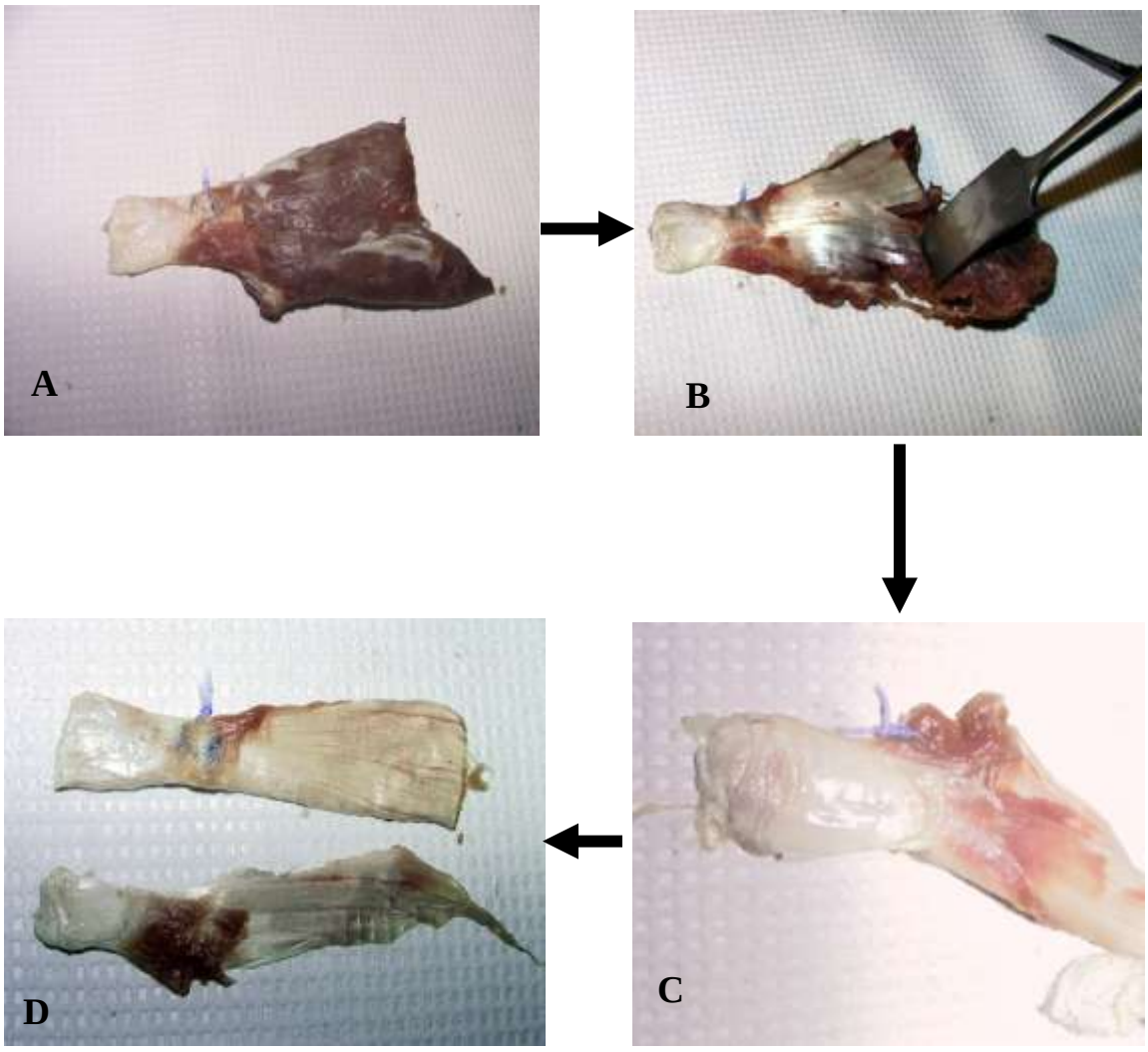

Figure 12: Figure showing the process by which the tendon grafts are harvested. A) Tendon with the attaching muscle is dissected out from the shoulder B) The muscles are scraped out C) Tendon stripped out of muscle D) The tendon is split longitudinally in to two grafts.

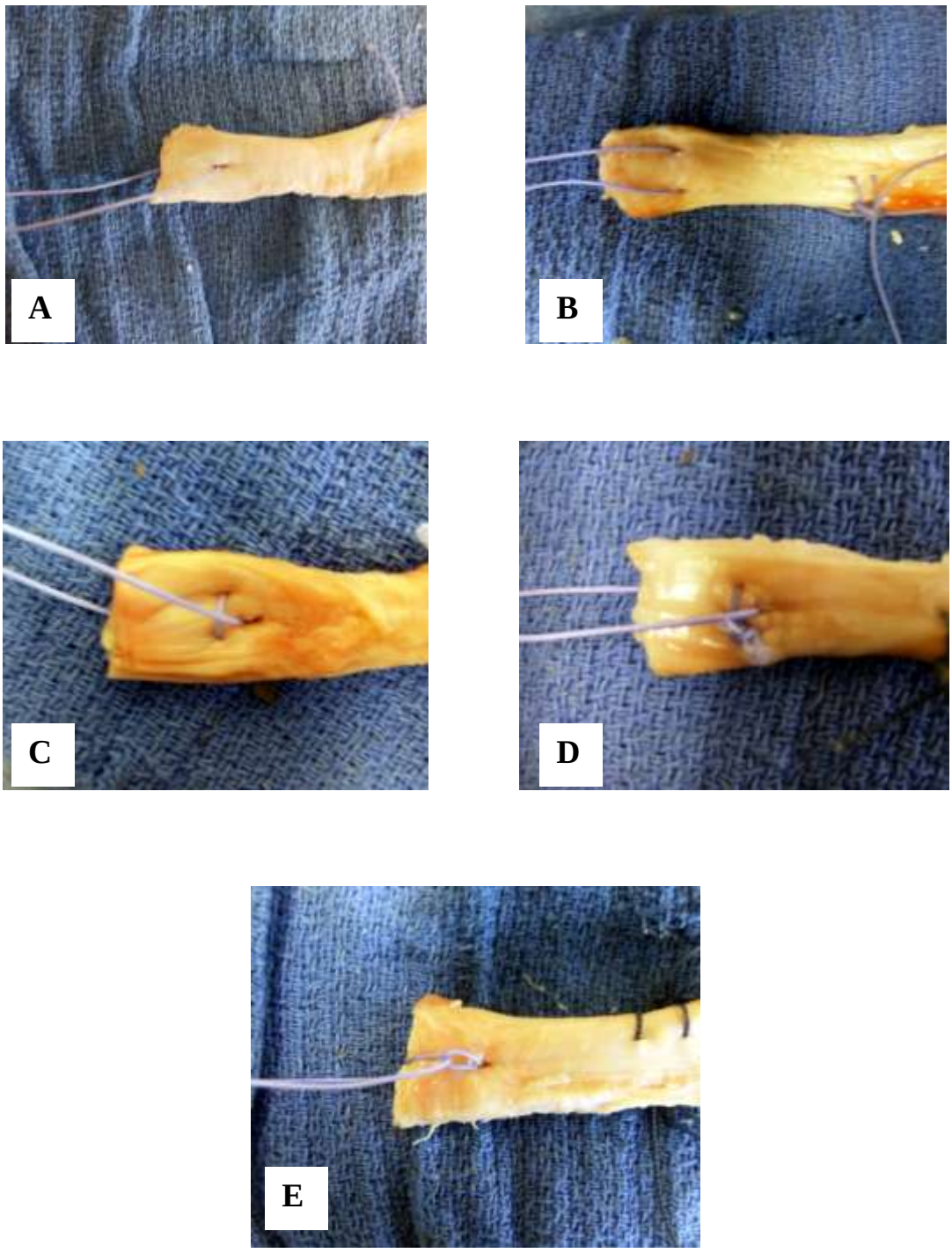

Figure 13: Figure showing the five different sutures placed.
A) Simple stitch, B) Mattress stitch C) Modified Mason-Allen (MMA) stitch D) Massive cuff (MAC) stitch and E) Lasso loop stitch.

Group 2: Forty-eight tendon grafts was used for evaluating the impact of tissue penetrator geometry on suture strength. Two different tissue penetrators namely the Chia Perc-Passer (DePuy Mitek, Raynham, MA) which has the smallest circular cross section and the Ideal Suture Passer (ISP) (DePuy Mitek, Raynham, MA) which has a mid-size circular cross section were used (Fig. 14). With each device, three different stitches namely, the mattress, MMA, and LL was placed. Thus we obtained a sample size of eight for each group. The suture were placed 0.5-cm from the distal tendon end by an experienced surgeon.

Group 3: The final thirty-six tendon grafts were used to evaluate the effect of bite size on the suture strength. These 36 grafts were equally divided among the five stitches: namely simple, mattress, MMA, MAC and lasso loop stitch. Thus we obtained a sample size of seven for each group. The suture in each graft was placed 1.0-cm from the distal tendon end. The stitches was placed using the Clever Hook (DePuy Mitek, Raynham, MA), tissue penetrator.

4.2.3 Biomechanical Testing

Biomechanical testing was carried out using the previous established method (Ma et al., 2004) in which the free end of the suture was tied around a fixed metal bar which is attached to a 10 KN load cell (Fig. 15). This setup was utilized so as to exclude the tendon-bone interface and thus this process evaluates the strength of the suture-tendon interface only (Gerber et al., 1994). The proximal tendon end was fixed in a custom

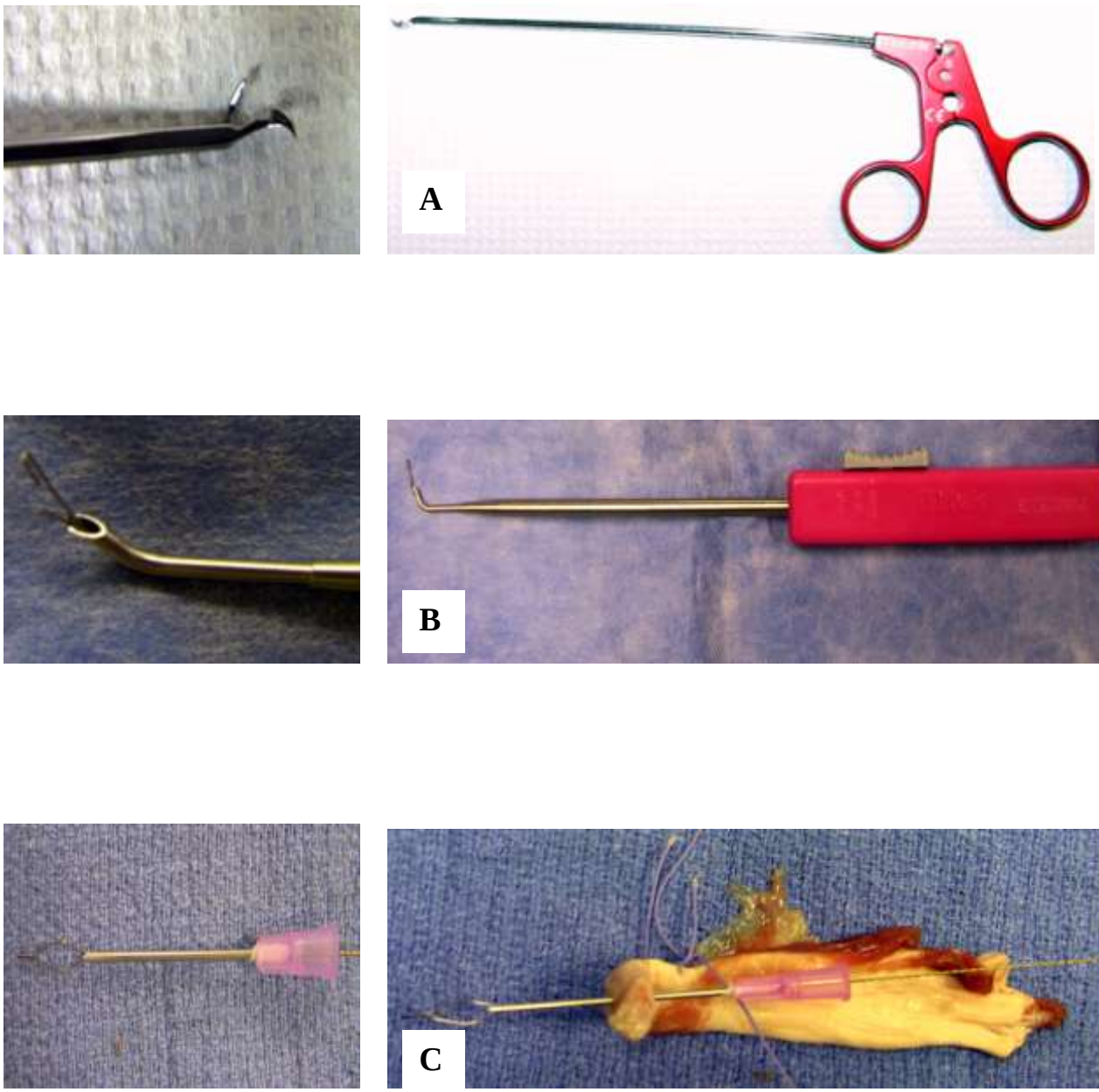

Figure 14: Three different tissue penetrators tested.
A) Clever hook, B) Ideal Suture Passer (ISP) and C) Chia Perc-Passer.

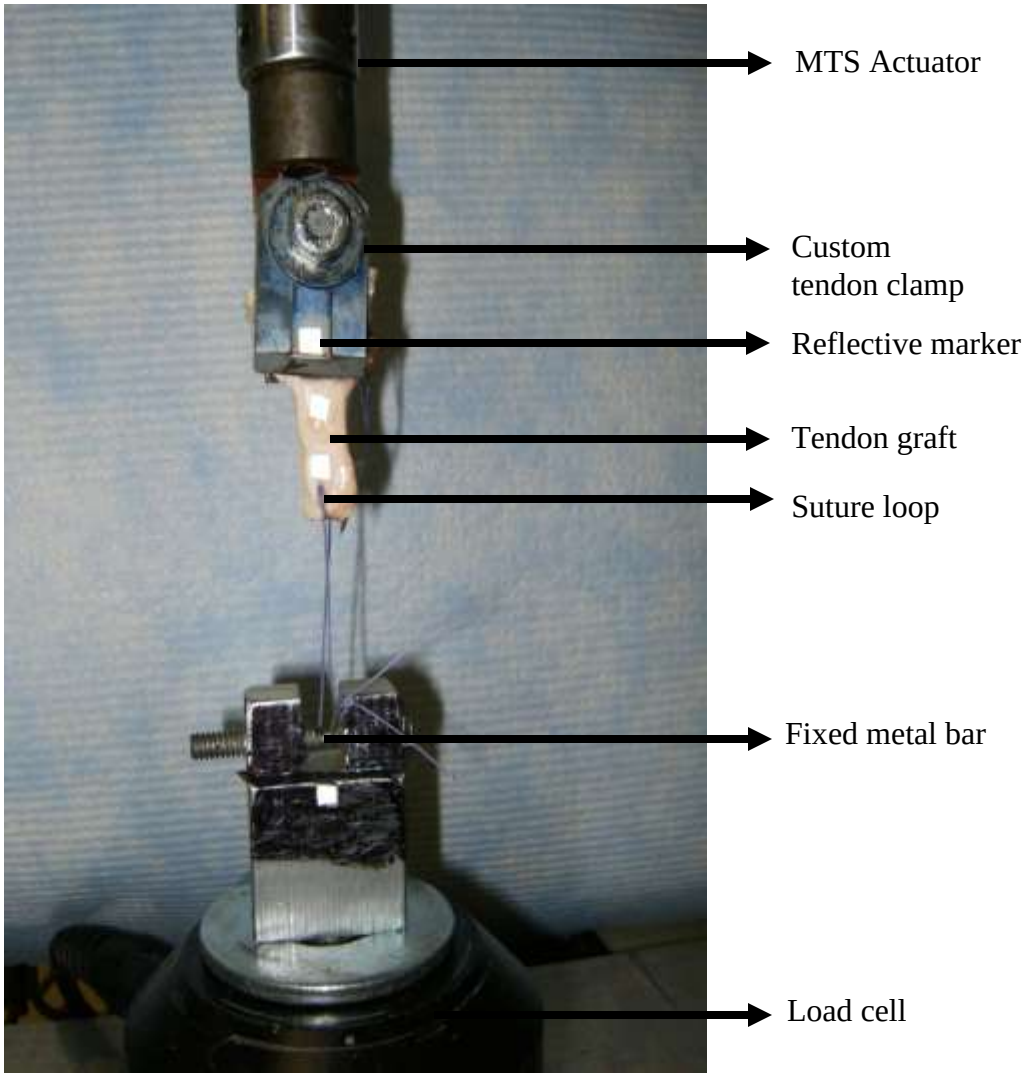

Figure 15: Jig used for testing suture strength

tendon clamp on an uniaxial 858 Mini-Bionix uniaxial servohydraulic Materials Testing System (MTS Systems Corp., Eden Prairie, MN, USA).

Four self-adhesive 2-mm-diameter retro-reflective passive markers (Qualysis Inc., East Windsor, CT); one at the suture-tendon interface, one at the clamp-tendon interface, one on the clamp and one on the metal bar adjacent to the suture loop were placed in each tendon. An infrared camera (Qualysis Inc., East Windsor, CT) having a resolution of +/- 0.05mm connected to a computer running PCReflex (version 2.0; Motion Capture Software) for data acquisition was used. Markers were calibrated before each testing session by measuring the distance between the markers and the camera. The use of the video displacement measurement method prevents possible slippage of the clamp-tendon system from being included in the determination of displacement. The data was sampled at frequency of 120 Hz to measure the relative displacement of the tendon and the suture on the basis of the marker displacements.

4.2.3.1 Cyclic Loading Test

Each tendon graft underwent a cyclic loading test in which its performance under repeated loading conditions was examined. A 5-N preload was applied to pretension the specimen after which the tendon was cyclically loaded under force control from 5 to 20 N at 0.25 Hz for twenty cycles with use of a half-sinusoidal waveform. The 20-N upper limit for twenty cycles was chosen based on the initial trials performed. Elongation and peak-to-peak displacement was determined in the cyclic loading test. Elongation is defined as the difference in y-displacement between the first cyclic peak and the

twentieth cyclic peak. Peak-to-peak displacement is defined as the average of the local minimum to maximum of the eighteenth, nineteenth, and twentieth cycles (Fig. 16).

4.2.3.2 Load to Failure/ Tensile Test

Following cyclic loading, each tendon specimen was loaded to failure under displacement control at a rate of 1 mm/sec and sampled at a frequency of 100 Hz. Actuator force and displacement were recorded using the MTS TestStar software. Following testing, the actuator load and displacement data were transferred to Excel software (Microsoft Corporation, Seattle, WA) to create load-displacement curves. From the load-displacement curves, load to failure of each tendon graft was obtained (Fig. 17). The peak force was considered as the load to failure. Also the failure mechanism (suture breakage or pull-out) for each specimen was recorded.

4.2.4 Statistical Analysis

A two-way ANOVA was carried out to find the effect of the bite size and the type of suture . Again two-way ANOVA was carried out to compare the effect of instrument geometry and the type of suture used on the biomechanical properties. Statistical analysis of elongation, peak-to-peak displacement and load to failure was performed with a significance level of $\alpha = 0.05$.

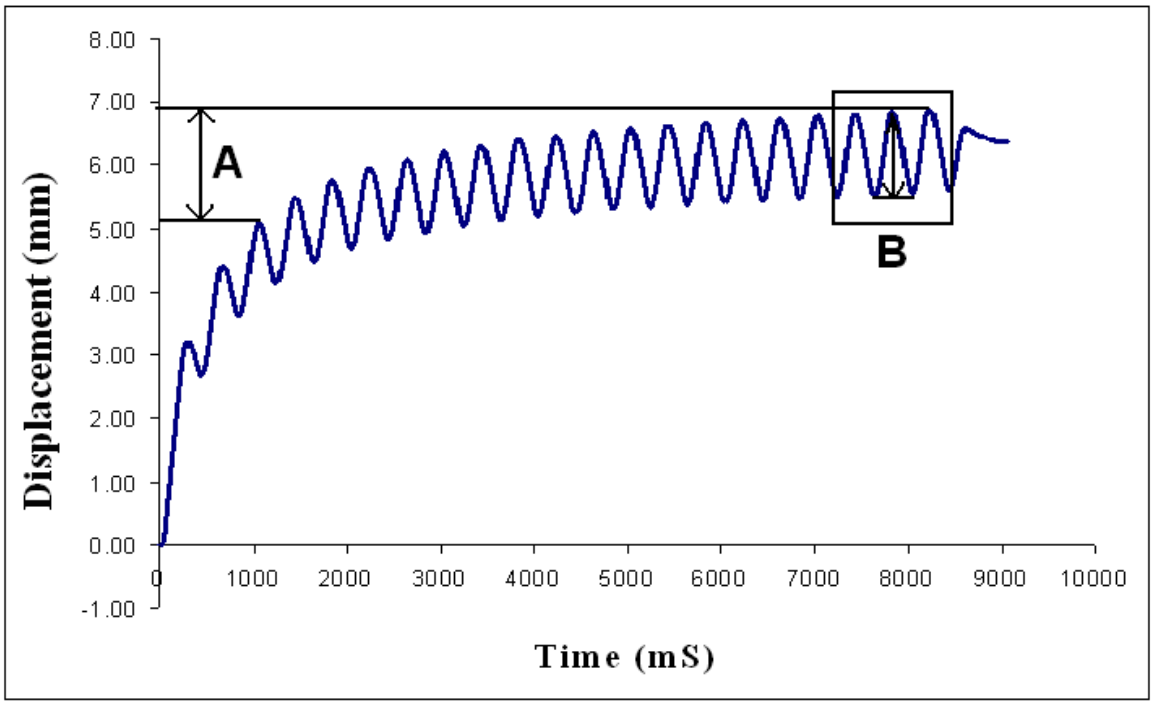

Figure 16: Graph showing a cyclic loading test.
A) cyclic elongation B) peak to peak displacement

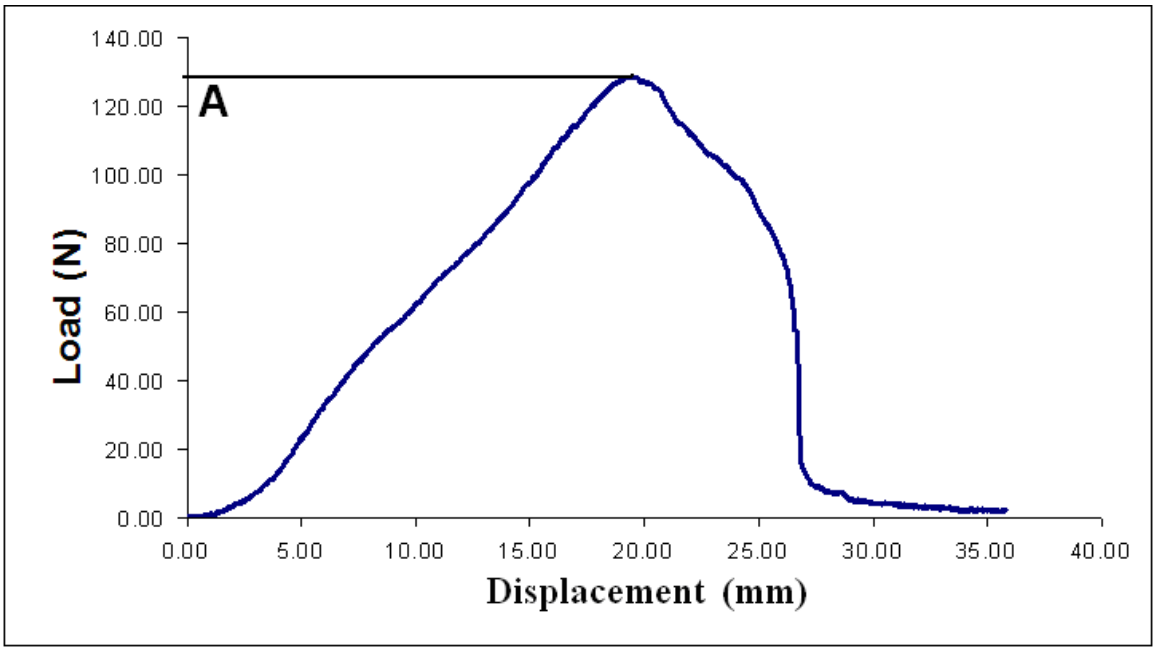

Figure 17: Graph showing a load to failure test.
A) maximum load to failure

CHAPTER 5

RESULTS

5.1 Calcar Fixaion and Stability

The results obtained from the biomechanical testing are shown in Table 1. The results indicate that the medial comminuted group without calcar fixation (short E-hole screws) produced the lowest values of load to failure, energy to failure and stiffness. Each of these values increased, in ascending order, for the group with medial comminution and good calcar fixation (long E-hole screws), non-comminution without calcar fixation, and non-comminution with calcar fixation. However this trend was not observed for the displacement at failure.

Table.1
Biomechanical properties of the construct tested (mean ± standard deviation)

Properties	MC without calcar fixation (N = 6)	MC with calcar fixation (N = 6)	NC without calcar fixation (N = 5)	NC with calcar fixation (N = 5)
Load to Failure (N)	491.39 ± 114.65	634.02 ± 224.32	981.19 ± 348.59	1235.58 ± 379.18
Energy to Failure (N*mm)	2014.09 ± 702.34	3000.04 ± 1390.2	4079.59 ± 2399.6	5369.01 ± 2843.2
Stiffness (N/mm)	104.76 ± 37.28	143.25 ± 65.42	156.91 ± 28.27	162.44 ± 31.38
Displacement at Failure (mm)	6.87 ± 1.90	7.66 ± 2.15	7.51 ± 1.88	7.76 ± 1.43

Regression model performed on biomechanical properties showed that BMD was not a statistically significant predictor for either outcome i.e. BMD did not have any significant effect on either comminution or calcar fixation ($p>0.05$). However, BMD significantly improved model fit and so it was included in the regression analyses.

The results showed that the medial comminuted specimens produced a much lower average load to failure (562 ± 169 N) than the non-comminuted specimens (1108 ± 363 N) (Fig. 18). Comminuted specimens had a drastic decrease of 49% average load to failure and this difference was found to be significant by both the ANOVA and regression analysis (p=0.015). While comparing the effect of calcar fixation, constructs with long E-hole screws withstood 27% more load than the constructs with short screws. The specimens with long E-hole screws (936 ± 301 N) yielded at significantly (p=0.002) higher average load than constructs with short E-hole screws (736 ± 231 N) (Fig. 19).

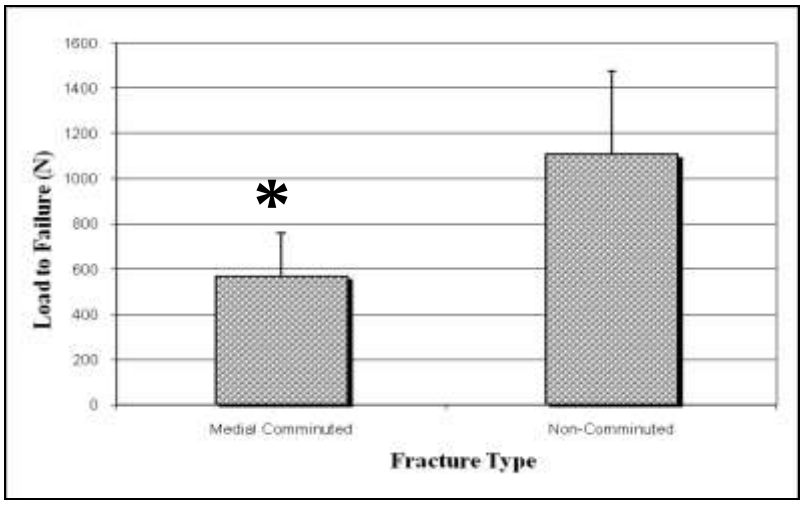

Figure 18: Comparison of average load to failure between comminuted and non-comminuted fracture trails. ***** Indicates significant difference ($p < 0.05$)

Similar results were obtained for energy to failure in which the medial comminuted specimens (2507 ± 1046 N*mm) had significant lower average energy as compared to the non-comminuted specimens (4724 ± 2620 N*mm) (p=0.013). This represents a decrease of 45% energy to failure(Fig. 20). In addition, constructs with long E-hole screws produced a higher average energy to failure (4185 ± 1616 N*mm) than short screws

(3047 ± 1550 N*mm) i.e. constructs with good calcar fixation absorbed 31% more energy than constructs without calcar fixation (Fig. 21).

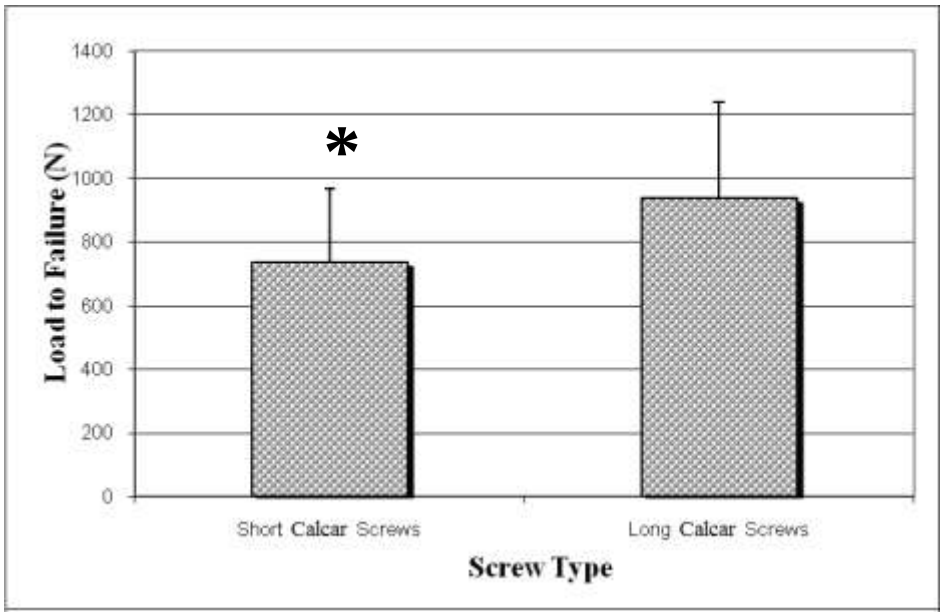

. Figure 19: Comparison of average load to failure between constructs with long and short calcar screws. ***** Indicates significant difference ($p < 0.05$)

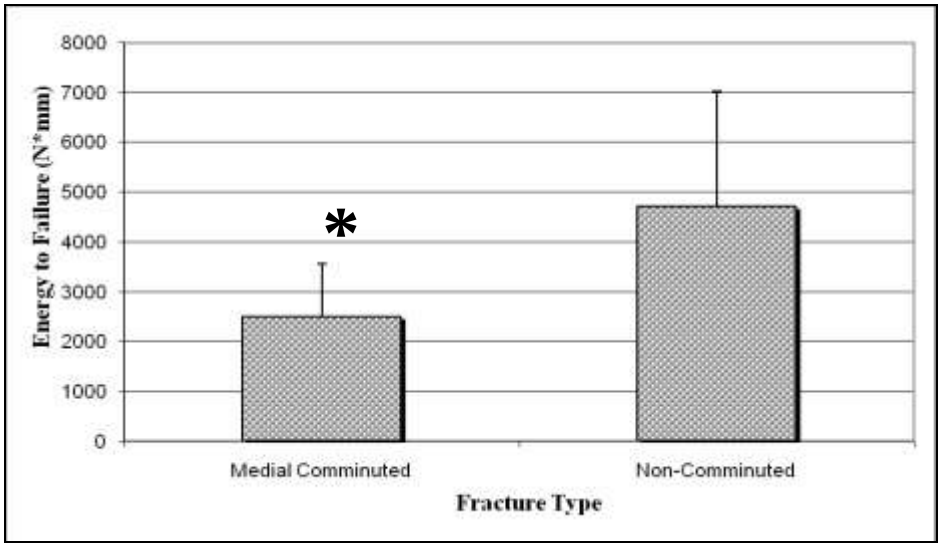

Figure 20: Comparison of average energy to failure between comminuted and non-comminuted fracture trails. ***** Indicates significant difference ($p < 0.05$)

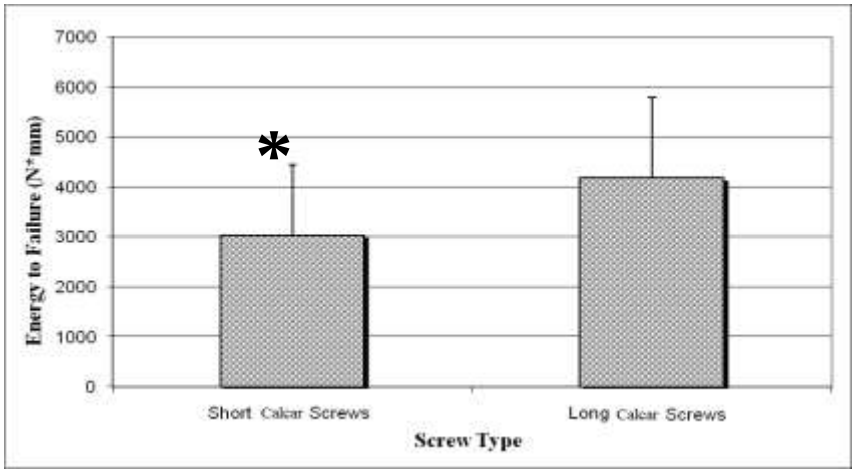

Figure 21: Comparison of average energy to failure between constructs with long and short calcar screws. ***** Indicates significant difference ($p < 0.05$)

In comparing the stiffness and displacement at failure between the four constructs, the regression analysis showed that neither calcar fixation nor lack of medial cortical contact had any significant effect ($p<0.05$) (Fig. 22, 23). Only an increasing trend in average stiffness was observed among the different test groups, with the comminuted specimens without calcar fixation having the lowest value and the specimens which lacked medial comminution and having calcar fixation having the highest stiffness. However no trend was found with regards to the displacement at failure.

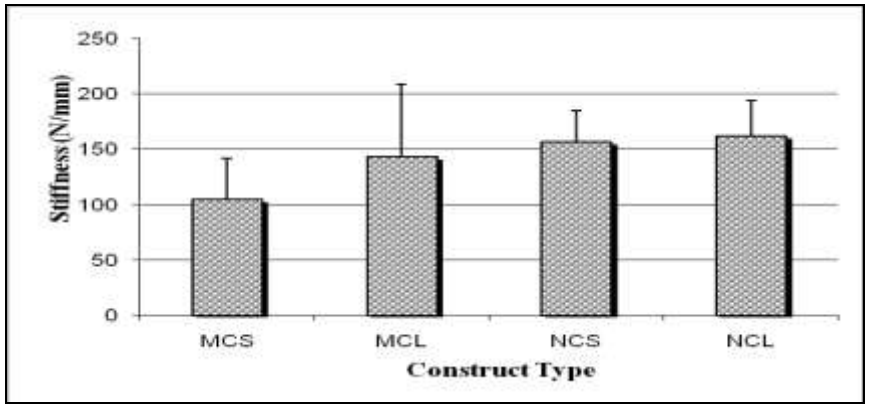

Figure 22: Comparison of stiffness between various constructs.

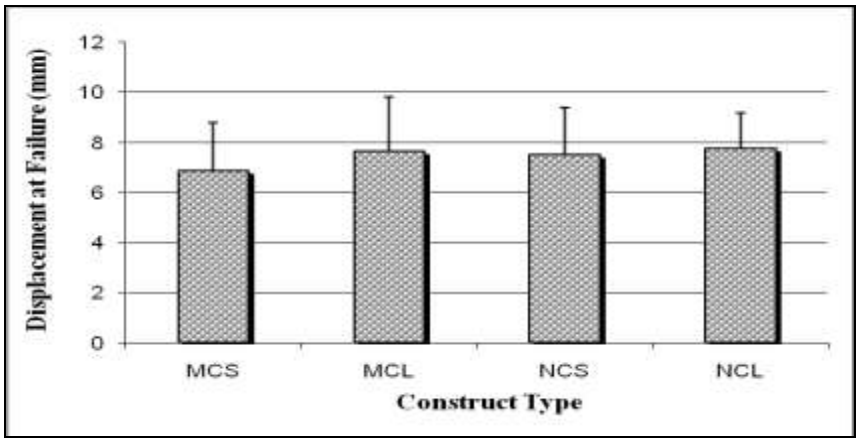

Figure 23: Comparison of displacement to failure between various constructs
MCS: Medial comminuted with short screws, MCL: Medial comminuted with long screw,
NCS: Non-comminuted with short screws, NCL: Non-comminuted with long screws

5.2 Mode of Failure

Regarding modes of failure, the comminuted fracture specimens were observed to deform immediately with the application of load, resulting in varus angulation and closure of the medial cortical defect. The load at which this closure occurred was considered as the load to failure. With further application of force, the closure was followed by shearing of the proximal humeral head along the medial fracture line and subsequent proximal screw pullout. At the completion of the test, the PHLP/comminuted fracture constructs were significantly weakened by loss of proximal fixation (Fig. 24).

However in two particular cases of comminuted fracture specimens, the humeral head first sheared along the medial fracture line and this was simultaneously accompanied by the varus angulation followed by subsequent proximal screw pullout (Fig 25). Also in three specimens, the PHLP plates had bent significantly at the end of the test (Fig. 26). However this bending phenomenon did not significantly affect the load or energy to failure values in these constructs.

Figure 24: Mode of failure in medial comminuted specimens.
Before loading (left) and after loading (right)

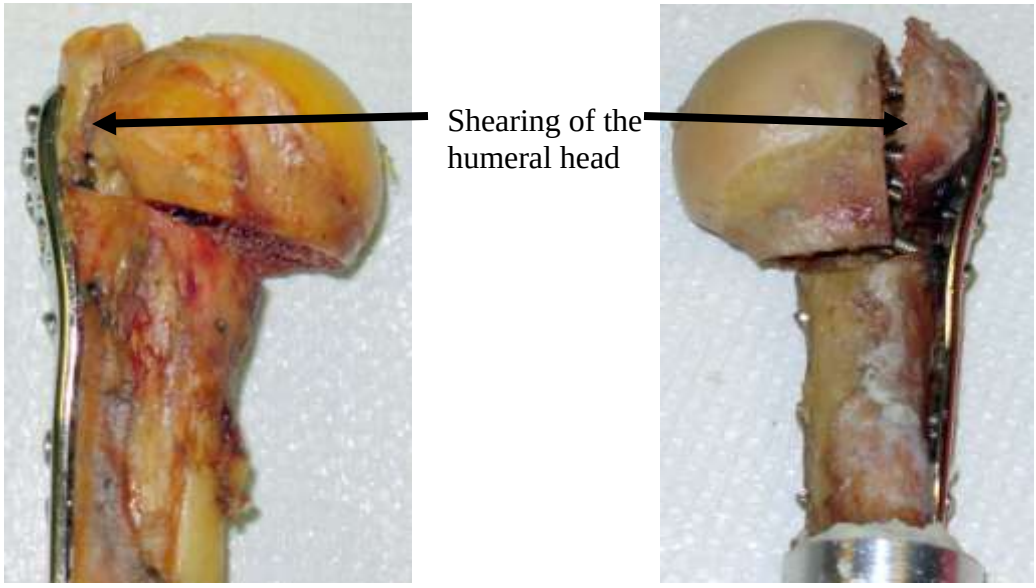

Figure 25: Figure showing the shearing of the humeral head

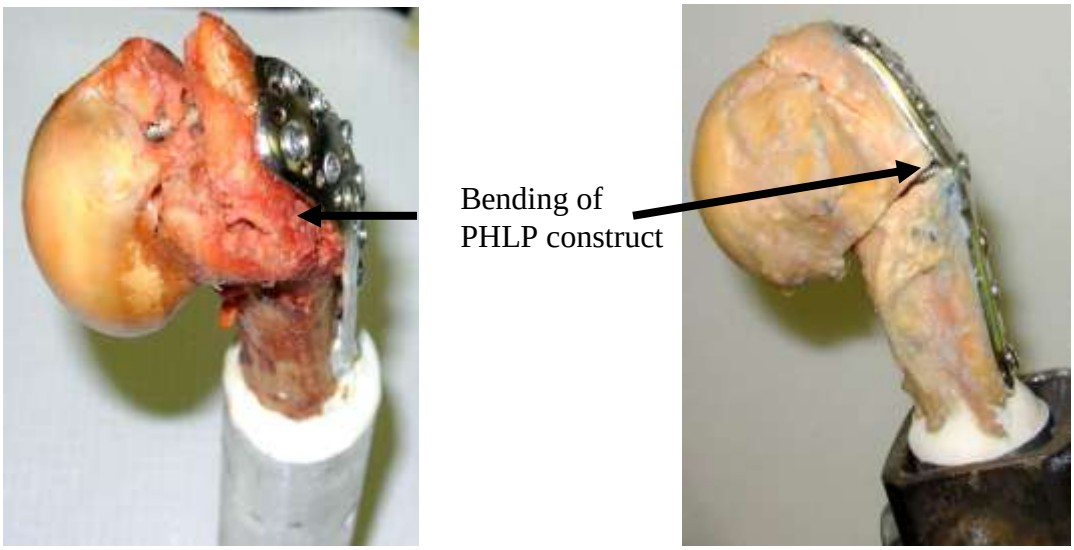

Figure 26: PHLP bent at the end of the test.

Figure 27: Mode of failure in non-comminuted specimens.
Before loading (left) and after loading (right)

In contrast to the comminuted fracture the non-comminuted fracture specimens did not show a clear pattern of failure (Fig. 27). In this case, the non-comminuted fracture specimens initially resisted displacement and angulation but with application of load the fracture line expanded, leading to failure of construct but with minimal varus angulation (Fig 26).

In three particular trials with in this group, the application of the load by the cupped cylinder caused an indentation on the humeral head (Fig. 28). In all these cases the load before failure was lower than that of the average failure loads in their respective groups. However this effect did not significantly affect energy to failure or the stiffness values within the group.

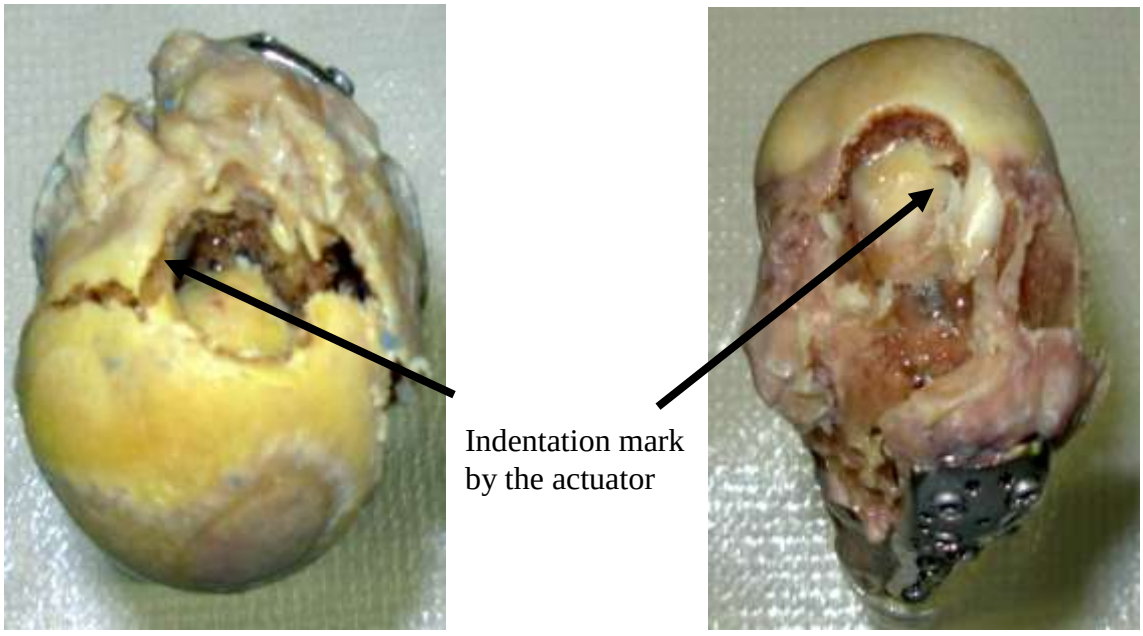

Figure 28: Figure showing the indentation caused by the actuator.

5.3 Evaluation of Lasso loop, Bite Size and the Instrument Size Used

When comparing the lasso loop with the other suture types, the lasso loop (56.14 ± 18.72 N) had 35% higher average load to failure than simple stitch (41.37 ± 24.92 N) although the difference was not statically significant (p=0.29). Also the mattress stitch (61.15 ± 27.6N) had similar average load to failure values with that of lasso loop stitch (p=0.62). Both MAC (150.33 ± 47.1 N) and MMA (114.22 ± 54.3 N) had significantly higher average load to failure than the lasso loop, mattress and simple stitch ($p<0.05$) (Fig. 29).

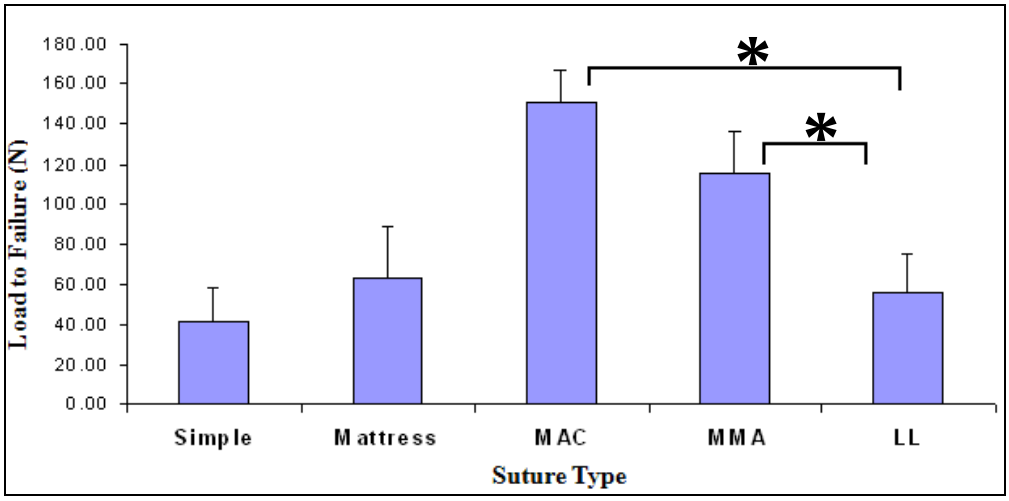

Figure 29: Graph comparing the average load to failure between the suture types.
***** Indicates significant difference ($p < 0.05$)

Table.2
Biomechanical properties of sutures tested using clever hook with 0.5-cm bite size (mean ± standard deviation)

Biomechanical Properties	Simple (N=8)	Mattress (N=8)	MAC (N=8)	MMA (N=8)	Lasso loop (N=8)
Load to Failure (N)	29.77 ± 27.48	44.91 ± 23.19	139.58 ± 45.13	100.13 ± 45.14	42.90 ± 15.20
Cyclic Elongation (mm)	1.32 ± 0.10	1.31 ± 0.09	1.37 ± 0.13	1.41 ± 0.17	1.39 ± 0.15
Peak to peak Displacement (mm)	1.14 ± 0.04	1.14 ± 0.08	1.17 ± 0.07	1.14 ± 0.07	1.18 ± 0.12

Table.3
Biomechanical properties of different sutures tested using clever hook with 1.0-cm bite size (mean ± standard deviation)

Biomechanical Properties	Simple (N=8)	Mattress (N=8)	MAC (N=8)	MMA (N=8)	Lasso loop (N=8)
Load to Failure (N)	52.96 ± 16.39	81.34 ± 32.08	162.61 ± 51.22	130.32 ± 56.90	69.38 ± 13.79
Cyclic Elongation (mm)	1.66 ± 0.15	1.70 ± 0.17	1.75 ± 0.19	1.77 ± 0.04	1.71 ± 0.22
Peak to peak Displacement (mm)	1.22 ± 0.06	1.26 ± 0.08	1.23 ± 0.08	1.21 ± 0.09	1.26 ± 0.08

When comparing the effect of bite size, the statistical analysis showed that the bite size had a significant effect as the load to failure in all the suture types (Table 2, 3). All the stitches had significantly higher load to failure at 1.0-cm purchase than the 0.5-cm purchase ($p=0.015$) (Fig. 30).

The cyclic test revealed that there was no significant difference ($p<0.05$) in either cyclic elongation or the peak to peak displacement between the different sutures at both 0.5-cm and 1.0-cm purchase (Fig. 31, 32). Although the cyclic elongation was greater (1.66 to 1.77 mm) in tendon grafts with 1-cm purchase than the 0.5-cm purchase grafts (1.31 to 1.41 mm). Similar results were observed in peak to peak displacement in which grafts with 1-cm purchase 1.14 to 1.18 mm while the 0.5-cm purchase grafts varied from 1.21 to 1.26 mm though this difference was not significant across the groups.

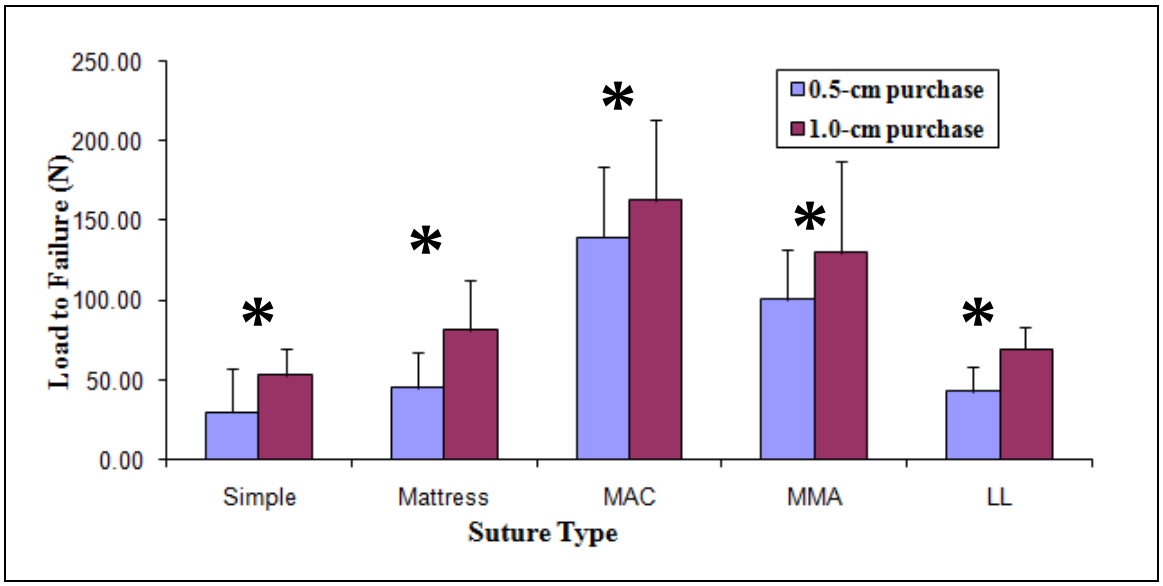

Figure 30: Graph comparing the load to failure between the suture types for the two purchase group. * Indicates significant difference ($p < 0.05$)

.

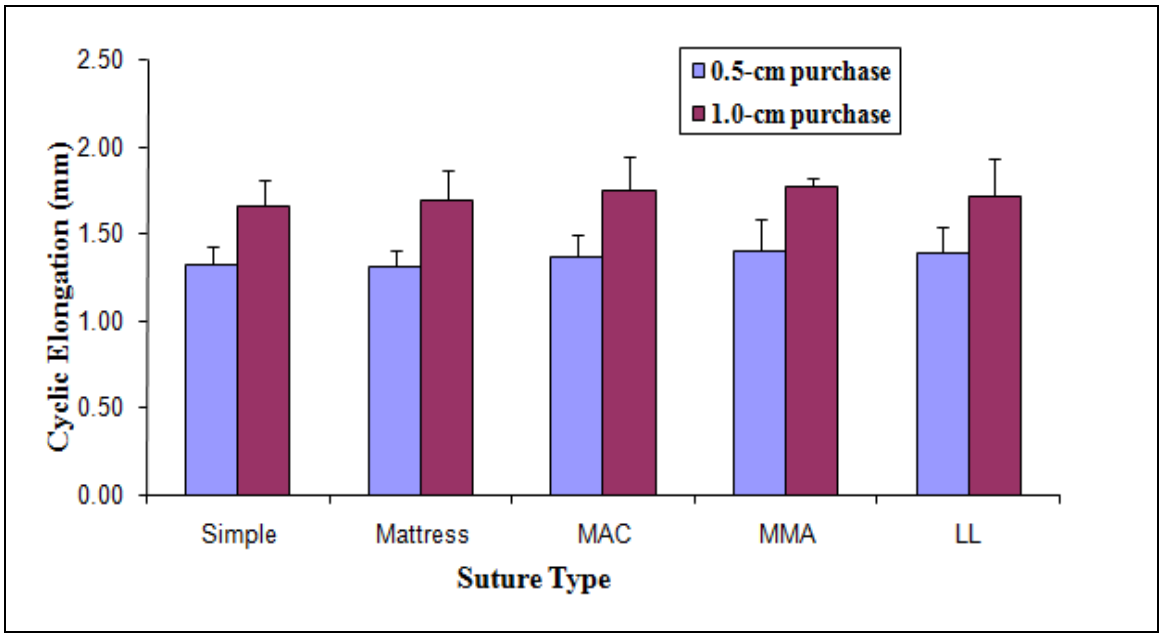

Figure 31: Graph comparing the cyclic elongation between the suture types for the two purchase group.

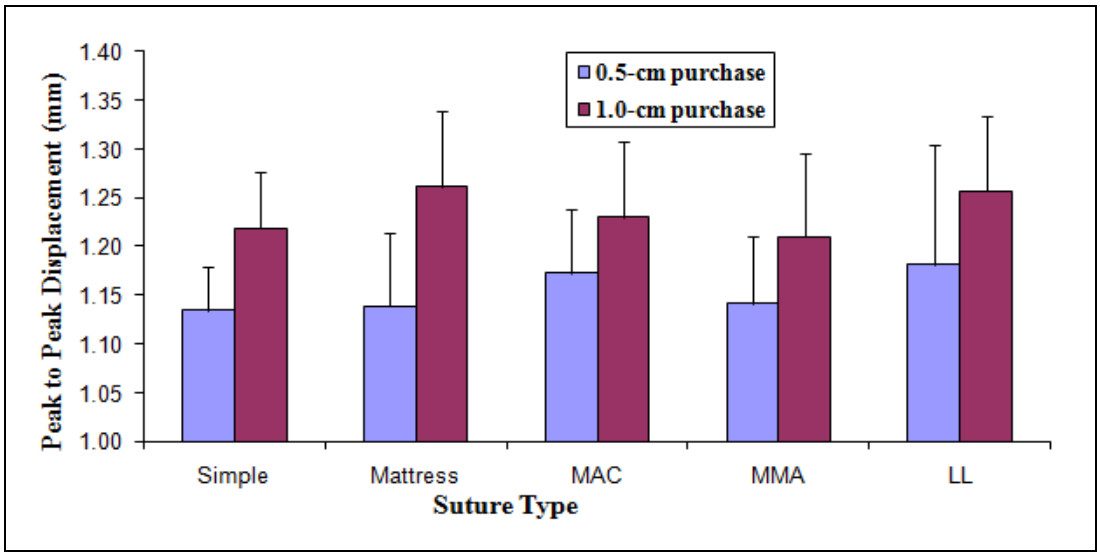

Figure 32: Graph comparing the peak to peak displacement between the suture types for the two purchase group.

Table.4
Biomechanical properties of sutures tested using chia perc-passer with 0.5-cm bite size (mean ± standard deviation)

Biomechanical Properties	Mattress (N=8)	MMA (N=8)	Lasso loop (N=8)
Load to Failure (N)	55.3 ± 21.39	124.0 ± 34.73	51.28 ± 21.34
Cyclic Elongation (mm)	1.38 ± 0.26	1.4 ± 0.2	1.39 ± 0.18
Peak to peak Displacement (mm)	1.19 ± 0.06	1.15 ± 0.08	1.19 ± 0.05

Table.5
Biomechanical properties of different sutures tested using Ideal Suture Passer with 0.5-cm bite size (mean ± standard deviation)

Biomechanical Properties	Mattress (N=8)	MMA (N=8)	Lasso loop (N=8)
Load to Failure (N)	41.06 ± 10.02	101.73 ± 36.38	49.87 ± 19.49
Cyclic Elongation (mm)	1.42 ± 0.22	1.43 ± 0.18	1.36 ± 0.13
Peak to peak Displacement (mm)	1.19 ± 0.05	1.17 ± 0.05	1.18 ± 0.09

The ANOVA showed that the load to failure was not affected by the different tissue penetrator used for all the three different sutures placed (p=0.18). Even though a trend of reduced strength with increasing tissue penetrator size was identified no significant difference was found in the average load to failure (Fig. 33). The average load to failure of the different stitches using the chia perc-passer was 55.3; 124.0; 51.28 N (mattress; MMA; lasso) while for the ISP was 41.6; 101.73; 49.87N and in case of clever hook it was 44.9; 100.1; 42.9N. When comparing the sutures placed, MMA had a significantly higher load to failure values than that of the lasso loop and the mattress stitch (p=0.001; p=0.001 respectively). Similar results were obtained for the cyclic tests in which the different tissue penetrator did not have any effect on either the cyclic elongation or the peak to peak displacement (p=0.23) (Fig. 34, 35).

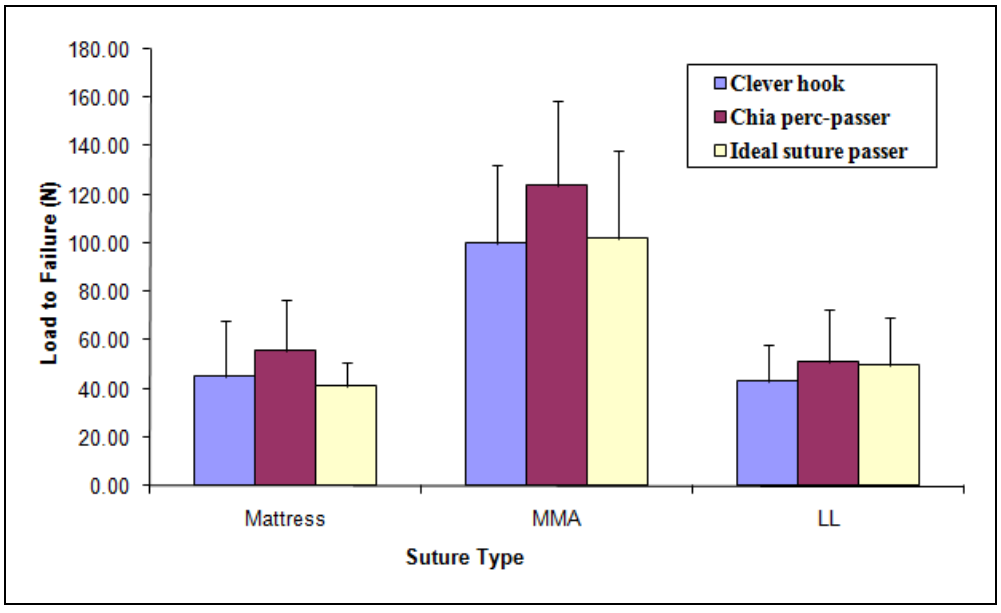

Figure 33: Graph comparing the load to failure between the suture types for the different tissue penetrator

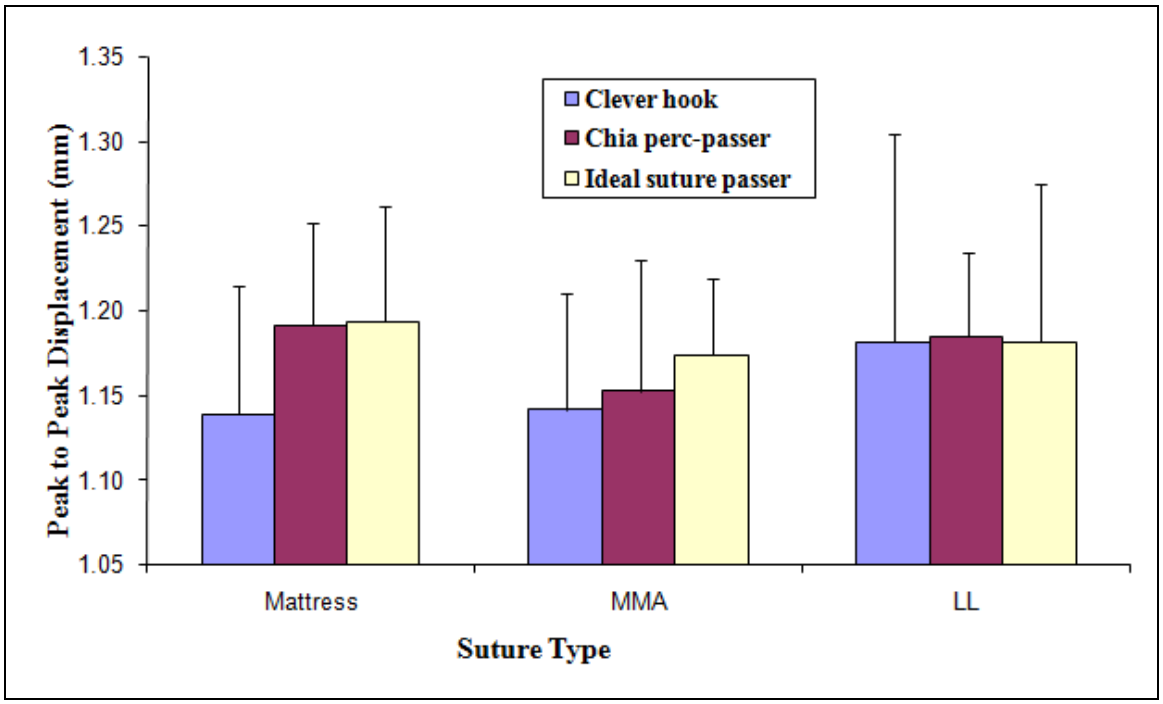

Figure 34: Graph comparing the peak to peak elongation between the suture types for the different tissue penetrator

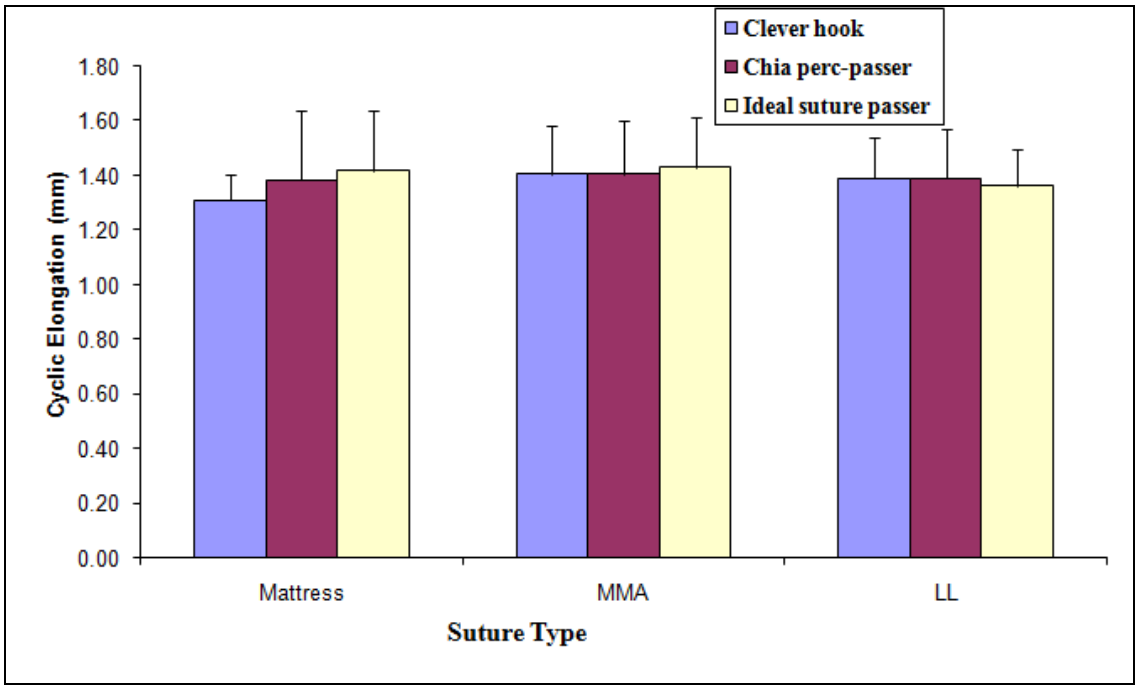

Figure 35: Graph comparing the cyclic elongation between the suture types for the different tissue penetrator

CHAPTER 6

DISCUSSION

6.1 Importance of Calcar Fixation

Proximal humerus fractures often presents difficulty in obtaining stable fixation mainly because of comminution and poor bone quality (Traxler et al., 2001). With the emergence of locked plating as most of the proximal humerus fractures are treated by this method it is important to understand the advantages and limitations of this treatment. Clinically, hardware failure and varus collapse continues to be a challenging problem. Hence in this study we created a fracture model to simulate a medial comminution, so as to evaluate its influence in aiding varus collapse.

Two important findings were identified: First, a lack of medial cortical contact significantly destabilizes proximal humerus fracture constructs. Clinically, residual calcar disruption can result from either an inadequate reduction or from medial communition. From the test results we see that the comminuted trails have a much significant lower load and energy to failure (by around 45%) than that of non-comminuted fracture specimens. This clearly demonstrates that proximal humerus fractures with a lack of cortical contact medially are at greater risk for varus collapse. Our findings are in agreement with previously published results (Chudik et al., 2005) in which they indicated that lack of medial cortical contact due to comminution may be a predictor of poor fixation outcome.

Second, restoration of stability with calcar fixation significantly improves fracture fixation strength. Fractures without calcar fixation (short E-hole screws) failing at significantly ($p < 0.05$) lower loads and energy to failure than those with calcar fixation (long E-hole screws) mirrors our hypothesis that greater stability and increased resistance to varus deformity is gained through use of long E-hole screws. Even with cortical contact medially, it is seen that placement of screws across the calcar region increased the load to failure values by around 26% (1235 N vs. 981 N). This was more prounced in case of fractures with medial comminution in which calcar fixation improved loads to failure by 29% (634 N Vs 491 N). Thus calcar fixation was significant independent of cortical contact medially.

When comparing the stiffness between the various construct, only a trend was observed between the comminuted and non-comminuted trails. Failure to identify a difference in stiffness in this study is expected, because the testing method and material was consistent for all trials. Stiffness depends on the entire experimental setup rather than any particular part of the testing material. As the variation in testing method and material is minimized, the difference in stiffness between the construct may be attributed to the differences in BMD in the humerus. Markus et al. (2005) showed that trabecular BMD of the humeral head has a significant effect on the pullout strength of cancellous screws. In our case as most of the locking screws and are placed in the humeral head, changes in BMD can affect the fixation stability of the PHLP construct thus affecting the stiffness.

With regard to the mode of failure, even though differences were observed between the two methods of fixation, both methods of fixation failed proximally in the head fragment, and the distal fixation to the shaft was not noticeably affected. These observations suggest that, the differences in the biomechanical properties between the specimens are mainly due to the differences in the proximal fixation in the PHLP constructs. As all the constructs had the same type of screws in the humeral head except the E-hole screws, we predict that these E- holes screws that are placed along the most inferior aspect are most likely responsible for the differences.

Our results were obtained using a fracture model where uniform and overall good fixation, that is, every hole in the locking plate was filled with a screw placed into the subchondral bone except for the variation in the E-hole screws so as to reduce confounding variables. Clinically, it is not unusual to have some of these screw holes left empty. Studies have shown that for locking plates for proximal humerus fractures, an average of five locking screws was only used (Ponce et al., 2007). Thus, the effect that calcar fixation screws have on stability of proximal humerus fractures likely would be even greater when some screw holes are not filled.

The locking plate may be adjusted slightly proximally or distally, and is often placed where it best fits the anatomy of the lateral cortex and greater tuberosity, without particular attention to the location of the screws in the proximal fragment. It has been found that placing the plate too proximal may lead to impingement of the plate on the acromion in abduction and placing the plate too distal may prevent the use of locked

screws of sufficient length, respectively (Fankhauser et al., 2005). So if the position of the plate is not chosen by ensuring that the inferomedial screws will be placed in the proper location, the screws may be easily misplaced and early mechanical failure may be more likely. In such cases the screw purchase plays an important role in the integrity of the construct. Though Liew et al (2000) found that the screw purchase was significantly greater when screws were placed in the medial subchondral bone they cautioned about not just relying on fixation in the superior humeral head. Thus a proper understanding of the bone-screw interface strength is necessary for the fixation of the proximal humeral fracture with the PHLP construct.

The limitation of the study includes the simple loading pattern which may not accurately reproduce the actual complex assortment of forces and factors encountered in vivo. Also our model failed to account for torsional forces, multidirectional forces, cyclic loading that may be encountered in actual scenario. However the biomechanical assessment we followed was consistent with a previous loading model and also the mode of failure we obtained in our testing construct was similar to that previously described in in-vivo trials (Esser et al., 1994), thus providing validation to our loading model.

6.2 Effect of Lasso loop, Bite Size and Instrument Geometry

Arthroscopic repair of the rotator cuff have become popular because of its lower morbidity and the ease of visualization (Wilson et al., 2002). Yet, concerns are raised regarding arthroscopic rotator cuff repair on the tendon fixation. Arthroscopic rotator cuff repairs are still limited to simple and horizontal mattress stitches because of the ease of suture placement (Burkhart et al., 1996). However we observe frequent re-tears in both these fixation method. Hence the main goal in arthroscopic rotator cuff repair has always been to obtain good tendon fixation to bone that is strong enough to allow for biologic healing as it has been widely accepted that the suture-tendon interface remains the probable site of failure of rotator cuff repair.

In this study we examined the effect of three different parameters with the aim of achieving better tendon fixation. First, we performed a biomechanical evaluation of a novel arthroscopic stitch, the lasso loop stitch in comparison to the other common stitches. Second, we analyzed the effect of increasing the bite size on the tendon holding strength and third, we studied the influence of the different geometry of the tissues penetrators that are commonly used in arthroscopic surgery on the tendon fixation.

The results of this study did not support our first hypothesis that the lasso loop stitch has comparable strength to MAC or MMA. Instead the biomechanical tests reveled that the lasso loop stitch had comparable strength with that of mattress stitch and had significantly less strength that of MAC and the MMA stitches. However, as predicted the lasso loop stitch (56.14 N) withstood higher average load to failure (35% increase) than

the simple stitch (41.37 N) even though this difference was not statistically significant. This indicates that the self-cinching effect or the "the strangulation" effect as described by Lafosse et al. (2006) created in the lasso loop stitch resulted in a better tendon fixation. Also as the lasso loop stitch had comparable strength to that of mattress stitch (63.12 N); the lasso loop could be used as alternative for the mattress stitch.

When comparing the other suture type, we found that the MAC (151.1 N) stitch had a significantly ($p<0.05$) higher load to failure values than the other stitches; even with that of MMA stitch (115.22 N). This observation was different from the previous studies by Ma et al., (2006) and Sileo et al. (2007) where they demonstrated that both MMA and MAC had similar load to failure. However our results from the cyclic loading test which did not demonstrate any significant difference among stitches with regard to peak-to-peak displacement or elongation was in agreement with the results obtained from Ma et al. (2006).

Our second hypothesis of different tissue penetrator geometry having influence in the tendon holding strength was also not supported by the experimental data. The data showed that the there was no influence on either load to failure or cyclic elongation or the peak to peak displacement by the three different tissue penetrators we used in this study. However we found the load to failure in almost all the suture type was highest with the chia perc-passer which had the smallest diameter, followed by the ISP which was a medium size tissue penetrator and finally the clever hook had the lowest load to failure value. Also in a study by Chokshi et al., (2006) they found that the durability of rotator

cuff repair under cyclic load depended upon the type of tissue penetrator used for suture passage through the tendon. Thus even though the failure loads were not significantly affected by the differences in tissue penetrator geometry in this study, it is recommend that a smaller diameter device be used for arthroscopic passage of sutures through the rotator cuff tendon so as to increase the tendon fixation.

The third hypothesis of bigger bite size will result in increased load to failure was supported by the biomechanical test data. The results clearly indicated a marked increase in failure load with 1.0-cm bite size when compared with that of the 0.5-cm bite irrespective of the suture used. This suggests that for a good tendon fixation, one need to have a better bite size. Also previous study has demonstrated that a larger tissue purchase improved the footprint coverage (Harryman et al., 2000). However one has to be critical about the bite size for the suture placement as it as known fact that the tendon thickness decreases proximally as it give rise to the muscle attachments.

The main focus of this study was to test the strength of the suture-tendon interface i.e., the tissue-holding strength of the stitch where clinical failures are reported. We utilized the experimental setup described by Ma et al. (2006), in which the sutures were tied around a metal bar to exclude the suture-bone or bone-anchor interfaces. Hence the observed mode of failure in the entire specimen was the suture tearing out of the tendon which was similar to the failure mode obtained in previous studies (Ma et al., 2006).

The limitations of the study include the use of sheep tendons. Though studies have shown that sheep rotator cuff tendons resemble human rotator cuff tendons in size, shape, and microstructure they are different from the degenerated tendons seen in human shoulders with chronic rotator cuff tears. However the sheep infraspinatus tendon has been shown to be a good model and has been used extensively for the evaluation of rotator cuff tendon repairs (Gerber et al., 1998; Lewis et al., 2001). Another limitation of the study was that all stitches were placed in an open environment, as opposed to arthroscopically. Also this study does not include the potentially confounding variables such as the tendon-bone or the bone-anchor interfaces found in physiological conditions.

As this study demonstrates that cinching effect in the stitch could increase the suture strength, our future work will involve testing other novel cinching suture techniques like mattress-lasso and double-cinch stitches. Also, we will be testing more specimens per each suture group so as to demonstrate a significant difference between the lasso loop stitch and the simple stitch. Apart from this the future work will involve testing the performance of the sutures including the tendon-bone interface and the tendon-anchor interface.

LIST OF REFERENCES

1) Agel J, Jones CB, Sanzone AG, Camuso M, Henley MB. Treatment of proximal humeral fractures with polarus nail fxation. Journal of shoulder and elbow surger, 2004; 13:191–195.

2) Baron JA, Karagas M, Barrett J, Kniffin W, Malenka D, Mayor M, Keller RB. Basic epidemiology of fractures of the upper and lower limb among Americans. Epidemiology 1996; 7:612-18.

3) Benegas E, Zoppi Filho A, Ferreira Filho AA, Ferreira Neto AA, Negri JH, Prada FS, Zumiotti AV. Surgical treatment of varus malunion of the proximal humerus with valgus osteotomy. Journal of shoulder and elbow surgery, 2007; Jan-Feb 16(1):55-9.

4) Bernard J, Charalambides C, Aderinto J, Mok D. Early failure of intramedullary nailing for proximal humeral fractures Injury, 2000; 31:789–792.

5) Burkhart SS, Diaz Pagàn JL, Wirth MA, Athanasiou KA. Cyclic loading of anchor-based rotator cuff repairs: confirmation of the tension overload phenomenon and comparison of suture anchor fixation with transosseous fixation. Arthroscopy, 1997; 13(6): p. 720-4.

6) Charalambous CP, Siddique I, Valluripalli K, Kovacevic M, Panose P, Srinivasan M, Marynissen H. Proximal humeral internal locking system (PHILOS) for the treatment of proximal humeral fractures. Archives of orthopaedic and trauma surgery, 2007; 127:205—210.

7) Chokshi BV, Kubiak EN, Jazrawi LM, Ticker JB, Zheng N, Kummer FJ, Rokito AS. The effect of arthroscopic suture passing instruments on rotator cuff damage and repair strength. Bulletin of the Hospital for Joint Diseases Orthopaedic Institute, 2006; 63(3-4):123-5.

8) Chudik SC, Weinhold P, Dahners LE. Fixed-angle plate fixation in simulated fractures of the proximal humerus: a biomechanical study of a new device. Journal of shoulder and elbow surgery, 2003; Nov-Dec, 12(6):578-88.

9) Cummins, C.A. and G.A. Murrell, Mode of failure for rotator cuff repair with suture anchors identified at revision surgery. Journal of shoulder and elbow surgery, 2003; 12(2): p. 128-33.

10) Diederichs G, Korner J, Goldhahn J, Linke B. Assessment of bone quality in the proximal humerus by measurement of the contralateral site: a cadaveric analysis. Archives of orthopaedic and trauma surgery 2006; 126: 93—100.

11) Edwards SL, Wilson NA, Zhang LQ, Flores S, Merk BR. Two-Part Surgical Neck Fractures of the Proximal Part of the Humerus. The Journal of Bone and Joint Surgery, 2006; Volume 88-A Number 10 October.

12) Egol KA, Kubiak EN, Fulkerson E, Kummer FJ, Koval KJ. Biomechanics of locked plates and screws. Journal of orthopaedic trauma, 2004; 18:488—493.

13) Gardner MJ, Griffith MH, Dines JS, Briggs SM, Weiland AJ, Lorich DG. The extended anterolateral acromial approach allows minimally invasive access to the proximal humerus. Clinical orthopaedics and related research 2005(434); p. 123-9.

14) Gardner MJ, Weil Y, Barker JU, Kelly BT, Helfet DL, Lorich DG. The importance of Medial Support in Locked Plating of Proximal Humerus. Journal of orthopaedic trauma, 2007; Vol 21:185-191.

15) Gazielly, D.F., P. Gleyze, and C. Montagnon, Functional and anatomical results after rotator cuff repair. Clinical orthopaedics and related research, 1994(304); p. 43-53.

16) Gerber C, Werner CM, Vienne P. Internal Fixation of Complex fractures of the Proximal Humerus The Journal of bone and joint surgery, 2004; Aug, 86(6): 848-55.

17) Gerber C, Hersche O, Berberat C. The clinical relevance of posttraumatic avascular necrosis of the humeral head. Journal of shoulder and elbow surgery, 1998; 7(6): p. 586-90.

18) Harryman DT 2nd, Mack LA, Wang KY, Jackins SE, Richardson ML, Matsen FA 3rd. Repairs of the rotator cuff. Correlation of functional results with integrity of the cuff. The Journal of bone and joint surgery, 1991; 73(7): p. 982-9.

19) Hepp P, Lill H, Bail H, Korner J, Niederhagen M, Haas NP, Josten C, Duda GN. Where should implants be anchored in the humeral head?. Clinical orthopaedics and related research, 2003; 415:139—147.

20) Hertel R. Fractures of proximal Humerus in Osteoporotic bone. Osteoporosis international, 2005; Mar 16 Suppl 2:S65-72. Epub 2004 Oct 30

21) Hintermann, B., H.H. Trouillier, and D. Schafer, Rigid internal fixation of fractures of the proximal humerus in older patients. The Journal of bone and joint surgery, 2000; 82(8): p. 1107-12.

22) Jansen T, Thorns C, Oestern HJ. Anatomy of the shoulder joint, Journal of Athletic Training, 2001; Mar 126(3):168-76.

23) Kannus P, Palvanen M, Niemi S, Parkkari J, Jarvinen M, Vuori I. Osteoporotic fractures of the proximal humerus in elderly Finnish persons: Sharp increase in 1970–1998 and alarming projections for the new millennium. Acta orthopaedica Scandinavica, 2000; 71:465–470.

24) Karduna AR. Kinematics of the glenohumeral joint: influences of muscle forces, ligamentous constraints, and articular geometry. Journal of orthopaedic research, 1996; 14(6):986–93

25) Kelkar R, Wang VM, Flatow EL, Newton PM, Ateshian GA, Bigliani LU, Pawluk RJ, Mow VC. Glenohumeral mechanics: A study of articular geometry, contact, and kinematics, Journal of shoulder and elbow surgery, 2001; Jan-Feb;10(1):73-84.

26) Klein MA, Miro PA, Spreitzer AM, Carrera GF. MR Imaging of the Normal Sternoclavicular Joint: Spectrum of Findings, American journal of roentgenology, 1995; Aug 165(2):391-3.

27) Koval KJ, Blair B, Takei R, Kummer FJ, Zuckerman JD. Surgical neck fractures of the proximal humerus: a laboratory evaluation often fixation techniques. The Journal of trauma, 1996; 40(5): p. 778-83.

28) Kronberg M, Broström LA, Söderlund V. Retroversion of the humeral head in the normal shoulder and its relationship to the normal range of motion Clin Orthop. 1990; 253:113-117.

29) Kwak SM, Brown RR, Resnick D, Trudell D, Applegate GR, Haghighi P. Anatomy, Anatomic Variations, and Pathology of the II - to 3- o'clock Position of the Glenoid Labrum, American journal of roentgenology, 1998; Jul 171(1):235-8.

30) Kyle RF, Cabanela ME, Russell TA, Swiontkowski MF, Winquist RA, Zuckerman JD, Schmidt AH, Koval KJ. Fractures of the proximal part of the femur. Instructional course lectures, 1995; 44: p. 227-53.

31) Lafosse L, Brozska R, Toussaint B, Gobezie R. The outcome and structural integrity of arthroscopic rotator cuff repair with use of the double-row suture anchor technique. Journal of shoulder and elbow surgery, 2007; 89(7): p. 1533-41.

32) Lafosse L, Van Raebroeckx A, Brzoska R. A new technique to improve tissue grip: the lasso loop stitch. Arthroscopy, 2006; 22(11): p. 1246 e1-3.

33) Lee TQ, Matsuura PA, Fogolin RP, Lin AC, Kim D, McMahon PJ. Arthroscopic suture tying: A comparison of knot types and suture materials. Arthroscopy, 2001; 17(4): p. 348-52.

34) Lewis CW, Schlegel TF, Hawkins RJ, James SP, Turner AS. The effect of immobilization on rotator cuff healing using modified Mason-Allen stitches: a biomechanical study in sheep. Biomedical sciences instrumentatiom, 2001; 37: 263-8.

35) Liew AS, Johnson JA, Patterson SD, King GJ, Chess DG. Effect of screw placement on fixation in the humeral head. Journal of shoulder and elbow surgery, 2000; 9(5): p. 423-6.

36) Ma CB, MacGillivray JD, Clabeaux J, Lee S, Otis JC. Biomechanical evaluation of arthroscopic rotator cuff stitches. The Journal of bone and joint surgery, 2004; Jun 86-A(6):1211-6.

37) Mac Gillivray, J.D. and C.B. Ma, An arthroscopic stitch for massive rotator cuff tears: the Mac stitch. Arthroscopy, 2004; 20(6): p. 669-71.

38) Meier RA, Messmer P, Regazzoni P, Rothfischer W, Gross T. Unexpected high complication rate following internal fixation of unstable proximal humerus fractures with an angled blade plate. Journal of orthopaedic trauma, 2006; 20(4): p. 253-60.

39) Neer CS II. Four-segment classification of proximal humeral fractures: Purpose and reliable use. Journal of shoulder and elbow surgery, 2002; 11:389—400.

40) Owsley KC, Gorczyca JT. Fracture Displacement and Hardware Migration after Open Reduction and Internal Fixation of Proximal Humerus Fractures. The Journal of bone and joint surgery, 2008; Feb 90(2):233-40

41) Parsons IM, Apreleva M, Fu FH, Woo SL. The effect of rotator cuff tears on reaction forces at the glenohumeral joint, Journal of Orthopaedic Research 2002; p. 439–446.

42) Plecko M, Kraus A. Internal fixation of proximal humerus fractures using the locking proximal humerus plate. Operative Orthopädie und Traumatologie, 2005; 17(1): p. 25-50.

43) Ponce BA, Ahluwalia RS, Mazzocca AD, Gobezie RG, Warner JJ, Millett PJ. Biomechanical and clinical evaluation of a novel lesser tuberosity repair technique in total shoulder arthroplasty. The Journal of bone and joint surgery, 2005; 87 Suppl 2: p. 1-8.

44) Porcellini G, Paladini P, Campi F, Paganelli M. Shoulder Instability and Related Rotator Cuff Tears: Arthroscopic Findings and Treatment in Patients Aged 40 to 60 Years, Arthroscopy: The Journal of Arthroscopic and Related Surgery, 2006; Vol 22, No 3 (March), pp 270-276.

45) Rees, J., J. Hicks, and W. Ribbans, Assessment and management of three-and four-part proximal humeral fractures. Clinical orthopaedics and related research, 1998; p. 18-29.

46) Sanchez-Sotelo J., Proximal Humerus Fractures, Clinical anatomy, 2006; Oct: 19(7):588-98.

47) Scheibel, M.T. and P. Habermeyer. A modified Mason-Allen technique for rotator cuff repair using suture anchors. Arthroscopy, 2003; 19(3): p. 330-3.

48) Schneeberger AG, von Roll A, Kalberer F, Jacob HA, Gerber C. Mechanical strength of arthroscopic rotator cuff repair techniques: an in vitro study. The Journal of bone and joint surgery, 2002; 84: 2152-60.

49) Sileo MJ, Ruotolo CR, Nelson CO, Serra-Hsu F, Panchal AP. A biomechanical comparison of the modified Mason-Allen stitch and massive cuff stitch in vitro. Arthroscopy, 2007; 23(3): p. 235-40, 240 e1-2.

50) Simon, R.S., Orthopaedic Basic Science, American Academy of Orthopaedic Surgeons, 1994

51) Smith J, Berry G, Laflamme Y, Blain-Pare E, Reindl R, Harvey E Percutaneous insertion of a proximal humeral locking plate: An anatomic study. Injury; 2007 Feb 38(2): 206-11.

52) Smith AM, Sperling JW, Cofield RH. Complications of operative fixation of proximal humeral fractures in patients with rheumatoid arthritis. Journal of shoulder and elbow surgery, 2005; 14(6): p. 559-64.

53) Steinbruck K. Epidemiology of sports injuries: 25-year analysis of sports orthopedic-traumatologic ambulatory care. Sportverletz Sportschaden, 1999; 13: 38 -52.

54) Terry GC, Chopp TM. Functional Anatomy of the Shoulder, Journal of Athletic Training, 2000; 35(3):248-255.

55) Warner JJ, Bowen MK, Deng X, Torzilli PA, Warren RF. Effect of joint compression on inferior stability of the glenohumeral joint Journal of shoulder and elbow surgery, 1999; Jan-Feb, 8(1):31-6.

56) Weinstein DM, Bratton DR, Ciccone WJ 2nd, Elias JJ. Locking plates improve torsional resistance in the stabilization of three-part proximal humeral fractures. Journal of shoulder and elbow surgery, 2006; 15(2): p. 239-43.

57) Whitelaw GP, Segal D, Sanzone CF, Ober NS, Hadley N. Unstable intertrochanteric/subtrochanteric fractures of the femur. Clinical orthopaedics and related research, 1990; p. 238-45.

58) Wilmanns C, Bonnaire F. Rotator cuff alterations resulting from humeral head fractures. Injury, 2002; Nov 33(9):781-9.

59) Wilson F, Hinov V, Adams G. Arthroscopic repair of full-thickness tears of the rotator cuff: 2- to 14-year follow-up. Arthroscopy. 2002; 18: 136-44.

APPENDIX

INSTITUTIONAL REVIEW BOARD APPROVAL

THE UNIVERSITY OF ALABAMA AT BIRMINGHAM

Institutional Review Board for Human Use

DATE: **February 2, 2007**

MEMORANDUM

TO: **Brent A. Ponce, M.D.**
Principal Investigator

FROM: Sheila Moore, CIP
Sheila Moore, CIP
Director, IRB

RE: Request for Determination—Human Subjects Research
IRB Protocol #N070119010 A Biomechanical Evaluation of Proximal Humerus Fractures Treated with Locking Plate Osteosynthesis: The Importance of Calcar Comminution and Fixation

An IRB Member has reviewed your application for Designation of Not Human Subjects Research for above reference proposal.

The reviewer has determined that this proposal is **not** subject to FDA regulations and is **not** Human Subjects Research. Note that any changes to the project should be resubmitted to the Office of the IRB for determination.

SM/lg

470 Administration Building
701 20th Street South
205.934.3789
Fax 205.934.1301
irb@uab.edu

The University of
Alabama at Birmingham
Mailing Address:
AB 470
1530 3RD AVE S
BIRMINGHAM AL 35294-0104